PHYSICAL REVIEW D **95,** 074005 (2017)

One-loop corrections to single spin asymmetries at twist-3 in Drell-Yan processes

A. P. Chen,[1,2] J. P. Ma,[1,2,3] and G. P. Zhang[4]

[1]*Institute of Theoretical Physics, Chinese Academy of Sciences, P.O. Box 2735, Beijing 100190, China*
[2]*School of Physical Sciences, University of Chinese Academy of Sciences, Beijing 100049, China*
[3]*Center for High-Energy Physics, Peking University, Beijing 100871, China*
[4]*Department of Modern Physics, University of Science and Technology of China, Hefei, Anhui 230026, China*

(Received 8 December 2016; published 5 April 2017)

We study single spin asymmetries at one-loop accuracy in Drell-Yan processes in which one of the initial hadrons is transversely polarized. The spin-dependent part of differential cross sections can be factorized with various hadronic matrix elements of twist-2 and twist-3 operators. These operators can be of even and odd chirality. In this work, the studied observables of asymmetries are differential cross sections with different weights. These weights are selected so that the observables are spin dependent and their virtual corrections are completely determined by the quark form factor. In the calculations of one-loop corrections we meet collinear divergences in the contributions involving chirality-odd and chirality-even operators. We find that all of the divergences can be correctly subtracted. Therefore, our results give an explicit example of QCD factorization at one loop with twist-3 operators, especially QCD factorization with chirality-odd twist-3 operators.

DOI: 10.1103/PhysRevD.95.074005

I. INTRODUCTION

Single transverse-spin asymmetry (SSA) can appear in high energy hadron-hadron collisions in which one of the initial hadrons is transversely polarized. For collisions with large momentum transfers one can make predictions by using QCD factorization, in which the perturbative and nonperturbative effects are consistently separated. It is well known that the cross sections with an unpolarized or longitudinally polarized hadron can be factorized with hadronic matrix elements of twist-2 operators. These matrix elements are the standard parton distribution functions. In the case of SSA the factorization is made with hadronic matrix elements of operators at twist-3, as shown in [1,2]. SSA is of particular interest in theory and experiment. Nonzero SSA indicates the existence of the nonzero absorptive part in scattering amplitudes. The matrix elements of twist-3 operators contain more information about inner structure of hadrons than those of twist-2 operators. Therefore, it is important to extract them from experiment.

In this work we study SSA in Drell-Yan processes. We construct two experimental observables, which are differential cross sections integrated over parts of phase space with weights. These weights are chosen so that the observables are proportional to the transverse spin. Using them one can extract the spin-dependent part of the full differential cross section and relevant twist-3 parton distributions. We study one-loop corrections of the constructed observables.

The two observables studied here receive contributions involving various parton distributions. Among them twist-3 parton distributions are unknown. It is important to know these twist-3 parton distributions. At tree level, only two twist-3 parton distributions are involved. They are quark-gluon-quark correlations inside hadrons. One is of transversely polarized hadron. Its existence implies that partons inside hadrons have nonzero orbital angular momenta. Another one is the correlation defined with a chirality-odd operator for an unpolarized hadron. The involved contribution is combined with the twist-2 transversity parton distribution, which is not well known. In hadronic processes there are usually significant corrections from next-to-leading order. With our results at one loop, the twist-3 parton distributions can be extracted from experimental results more accurately than with tree results. At one loop the twist-3 gluon distribution contributes. Knowing the one-loop correction, it can help to extract the twist-3 gluon distribution. Currently, the relevant experiment can be perform at the RHIC and Compass, where the transversely polarized proton beam or target is available.

SSA at tree level in Drell-Yan processes has been studied extensively. In [3–8] the effect of SSA has been studied in the case where the transverse momentum of the lepton pair is small and approaching 0. The effect is at the order of $\mathcal{O}(\alpha_s^0)$. For the case of the large transverse momentum SSA has been studied in [9–14], where the effect of SSA is at the order of $\mathcal{O}(\alpha_s)$. While calculations beyond tree level in QCD factorization at twist-2 are rather standard and many one-loop results exist, there are not many results of one-loop calculation with twist-3 factorization. For Drell-Yan processes there is only one work in [15] where one weighted differential cross section of SSA involving the twist-3 quark-gluon operator of [1,2] is calculated at one loop. For semi-inclusive deep inelastic scattering (SIDIS) different parts of one-loop results about SSA can be found in

[16–18]. A one-loop study of twist-3 factorization for DIS has been performed in [19].

Recently the complete twist-3 part of the hadronic tensor of the Drell-Yan process and of semi-inclusive DIS has been derived at the tree level $\mathcal{O}(\alpha_s^0)$ for the first time in [8,20], respectively. According to these results one can systematically construct weighted observables of SSA. An interesting finding in these works is that the twist-3 hadronic tensors contain a special part. This special part receives from higher orders of α_s the virtual correction, which is completely determined by that of the electromagnetic form factor of a quark. The results of higher-order correction of the quark form factor exist in the literature and can be easily recalculated at one loop. In this work, we construct two weighted differential cross sections. These two observables receive at tree level contributions only from the special part of the hadronic tensor. Therefore, the one-loop virtual correction to the two observables is well known. We then only need to calculate the real corrections to the observables. One can certainly construct observables whose tree-level results can receive contributions from other parts of the hadronic tensor besides or except the special part. In this case, the virtual correction needs to be calculated and the calculation can be complicated. We leave this for a study in the future.

In general twist-3 calculations are more complicated than those of twist-2. In the separation of nonperturbative and perturbative effects the gauge invariance of QCD should not be violated. In [21] it has been shown how the gauge invariance is maintained. In twist-3 factorization there is a special contribution called soft-gluon-pole contribution as shown in [2], in which one gluon is with zero momentum entering hard scattering. It should be noted that the momentum is not exactly 0. In fact the momentum of the gluon is in the Glauber region [13]. The soft-gluon-pole contribution is more difficult to calculate than others. Interestingly, it is shown in [22–24] that the soft-gluon-pole contribution at tree level is related to the corresponding twist-2 contribution at tree level. This simplifies the calculation of obtaining the soft-gluon-pole contribution. With these progresses twist-3 calculations can be done in a relatively straightforward way.

We calculate the one-loop correction of the two observables. The contributions to the observables can be divided into two parts. One part contains hadronic matrix elements of chirality-even operators, while another part involves chirality-odd operators. In calculating the chirality-even and chirality-odd contributions at one loop, one encounters infrared (I.R.), or collinear, divergences. The I.R. divergences are canceled in the sum of all contributions. The collinear divergences can be correctly factorized into hadronic matrix elements. The final results are finite. Unlike the collinear factorization at twist-2 for DIS and Drell-Yan processes, where the twist-2 factorization has been proven to hold at all orders, there is no proof of the collinear factorization at twist-3 at all orders. To show the factorization it is important to perform calculations beyond the tree level, because collinear and I.R. divergences do not appear at tree level. They appear at one-loop or higher orders. These divergences are potential sources to violate the factorization. Our work presented here gives an explicit example of twist-3 factorization at one loop. Especially, it is the first time in the case of the factorization involving chirality-odd operators at one loop.

Our paper is organized as follows. In Sec. II we introduce our notations and derive the tree-level results. In Secs. III and IV we give the one-loop corrections for the chirality-even and chirality-odd contributions, respectively. In these sections, we also perform the subtraction of the collinear contributions. The collinear singularities are subtracted into various parton distributions. In Sec. V we give our final results, which are finite. Section VI is our summary.

II. NOTATIONS AND TREE-LEVEL RESULTS

We consider the Drell-Yan process,

$$h_A(P_A,s)+h_B(P_B) \to \gamma^*(q)+X\to \ell^-(k_1)+\ell^+(k_2)+X, \tag{1}$$

where h_A is a spin-1/2 hadron with the spin vector s and the spin of h_B is 0 or averaged. We use the light-cone coordinate system, in which a vector a^μ is expressed as $a^\mu=(a^+,a^-,\vec{a}_\perp)=((a^0+a^3)/\sqrt{2},(a^0-a^3)/\sqrt{2},a^1,a^2)$. We introduce two light-cone vectors $l^\mu=(1,0,0,0)$ and $n^\mu=(0,1,0,0)$. Using the two vectors we define two tensors,

$$g_\perp^{\mu\nu}=g^{\mu\nu}-n^\mu l^\nu-n^\nu l^\mu, \qquad \epsilon_\perp^{\mu\nu}=\epsilon^{\alpha\beta\mu\nu}l_\alpha n_\beta,$$
$$\epsilon^{\alpha\beta\mu\nu}=-\epsilon_{\alpha\beta\mu\nu}, \qquad \epsilon^{0123}=1. \tag{2}$$

With the transverse metric $g_\perp^{\mu\nu}$ we have $a_\perp^\mu=g_\perp^{\mu\nu}a_\nu$ and $a_\perp^2=-a_\perp\cdot a_\perp=(a^1)^2+(a^2)^2$. The momenta of initial hadrons and the spin of h_A in the light-cone coordinate system are

$$P_A^\mu\approx(P_A^+,0,0,0), \qquad P_B^\mu\approx(0,P_B^-,0,0),$$
$$s^\mu=s_\perp^\mu=(0,0,s^1,s^2), \tag{3}$$

i.e., h_A moves in the z-direction with a large momentum. The invariant mass of the observed lepton pair is $Q^2=q^2=(k_1+k_2)^2$. The relevant hadronic tensor is defined as

$$W^{\mu\nu}=\sum_X\int\frac{d^4x}{(2\pi)^4}e^{iq\cdot x}\langle h_A(P_A,s),h_B(P_B)|\bar{q}(0)\gamma^\nu q(0)|X\rangle \times\langle X|\bar{q}(x)\gamma^\mu q(x)|h_B(P_B),h_A(P_A,s)\rangle. \tag{4}$$

We consider the case with $Q^2 \gg \Lambda^2_{\rm QCD}$. At leading power of Q^2, it is well known that $W^{\mu\nu}$ is factorized with twist-2 operators, which are used to define various standard parton distributions, whose definitions can be found in [25]. At this order $W^{\mu\nu}$ does not depend on the transverse spin $s_\perp$.

The $s_\perp$-dependence appears at the next-to-leading order of the inverse power of Q. At this order $W^{\mu\nu}$ can be factorized with twist-3 hadronic matrix elements or twist-3 parton distribution functions. We give the definitions of relevant twist-3 matrix elements in the following. For the transversely polarized h_A, there are two relevant twist-3 matrix elements, called Efremov-Teryaev-Qiu-Sterman (ETQS) matrix elements. They are defined as [1,2]

$$\int \frac{d\lambda_1 d\lambda_2}{4\pi} e^{-i\lambda_2(x_2-x_1)P_A^+ - i\lambda_1 x_1 P_A^+} \times \langle h_A|\bar\psi_i(\lambda_1 n) g_s G^{+\mu}(\lambda_2 n)\psi_j(0)|h_A\rangle = \frac{1}{4}[\gamma^-]_{ji}\tilde s_\perp^\mu T_F(x_1,x_2) + \frac{1}{4}[i\gamma_5\gamma^-]_{ji} s_\perp^\mu T_\Delta(x_1,x_2) + \cdots, \tag{5}$$

where $\cdots$ denotes irrelevant terms. The vector $\tilde s_\perp^\mu$ is defined as $\tilde s_\perp^\mu = \epsilon_\perp^{\mu\nu} s_{\perp\nu}$. In the above and the following, we suppress the gauge links between field operators at different points of the space-time for a short notation. These gauge links are important for making the definitions gauge invariant. The two twist-3 parton distribution functions defined in Eq. (5) have the property

$$T_F(x_1,x_2) = T_F(x_2,x_1), \qquad T_\Delta(x_1,x_2) = -T_\Delta(x_2,x_1). \tag{6}$$

One can define another two twist-3 distributions by replacing the field-strength tensor operator in Eq. (5) with the covariant derivative $D_\perp^\mu$. In addition to them, there are three twist-3 distributions defined with a product of two quark field operators. Two of them are given in [26], and one of them is defined in [20]. All of these mentioned twist-3 distributions can be expressed with the two defined in Eq. (5) [20,26]. Therefore, we only use $T_{F,\Delta}$ to express our results. We note here that $T_{F,\Delta}$ are defined with chirality-even operators.

There are four twist-3 distributions defined only with gluon fields [27]. One of them can be defined as

$$T_G^{(f)}(x_1,x_2)\tilde s^\mu = g_s \frac{i f^{abc} g_{\alpha\beta}}{P_A^+}\int \frac{dy_1 dy_2}{4\pi} e^{-iP_A^+(y_2(x_2-x_1)+y_1 x_1)} \times \langle h_A|G^{a,+\alpha}(y_1 n) G^{b,+\mu}(y_2 n) G^{c,+\beta}(0)|h_A\rangle. \tag{7}$$

The definition of $T_G^{(d)}$ is obtained by replacing if^{abc} with d^{abc}. Besides these two distributions $T_G^{(f,d)}$ the other two twist-3 distributions are defined by replacing $g_\perp^{\alpha\beta}$ with $\epsilon_\perp^{\alpha\beta}$ in Eq. (7). But the contributions with these two twist-3 distributions do not appear in calculations of our work. For the matrix elements with f^{abc} one has

$$T_G^{(f)}(x_1,x_2) = -T_G^{(f)}(-x_2,-x_1), \qquad T_G^{(f)}(x_1,x_2) = T_G^{(f)}(x_2,x_1). \tag{8}$$

Similar relations can be derived for distributions defined with d^{abc}. We use $T_G^{(f,d)}$ to give our results. The contributions involving these twist-3 distributions are in combination with the twist-2 parton distribution functions of h_B.

There are contributions to $W^{\mu\nu}$ involving hadronic matrix elements defined with chirality-odd operators. These contributions involve the twist-2 transversity distribution of h_A introduced in [28]. It is defined as

$$h_1(x)s_\perp^\mu = \int \frac{d\lambda}{4\pi} e^{-ix\lambda P_A^+}\langle h_A|\bar\psi(\lambda n)\gamma^+\gamma_\perp^\mu\gamma_5\psi(0)|h_A\rangle. \tag{9}$$

The twist-3 chirality-odd distributions of h_B appear in the contributions. For the unpolarized hadron h_B we can define

$$T_F^{(\sigma)}(y_1,y_2) = -\frac{2g_s}{d-2}\int \frac{d\xi_1^+ d\xi_2^+}{4\pi} e^{-i\xi_1^+ y_1 P_B^- - i\xi_2^+(y_2-y_1)P_B^-} \times \langle h_B|\bar q(0)(i\gamma_{\perp\mu}\gamma^-)G^{-\mu}(\xi_2^+ l) q(\xi_1^+ l)|h_B\rangle \tag{10}$$

with d as the dimension of the space-time. Another twist-3 chirality-odd distribution, called $e(x)$, for the unpolarized hadron is defined with the operator $\bar\psi\psi$. With the equation of motion one can relate $e(x)$ to $T_F^{(\sigma)}$ [29–31].

The complete result for the twist-3 contribution of $W^{\mu\nu}$ in the considered case at the leading order of α_s has been derived in [8]. It is

$$W^{\mu\nu} = \frac{1}{2N_c}\Bigg\{-T_F^{(\sigma)}(y,y)h_1(x) \times \left[\frac{1}{2}\frac{\partial\delta^2(q_\perp)}{\partial q_\perp^\rho}(g_\perp^{\mu\rho}\tilde s_\perp^\nu + g_\perp^{\nu\rho}\tilde s_\perp^\mu - g_\perp^{\mu\nu}\tilde s_\perp^\rho) + \frac{\delta^2(q_\perp)}{P_B\cdot q}(P_B^\mu \tilde s_\perp^\nu + P_B^\nu \tilde s_\perp^\mu)\right] + \bar q(y) T_F(x,x)\left[\frac{\delta^2(q_\perp)}{P_A\cdot q}(P_A^\mu \tilde s_\perp^\nu + P_A^\nu \tilde s_\perp^\mu) + g_\perp^{\mu\nu}\frac{\partial\delta^2(q_\perp)}{\partial q_\perp^\rho}\tilde s_\perp^\rho\right]\Bigg\} + \mathcal{O}(\alpha_s), \tag{11}$$

where $\bar q(y)$ is the antiquark distribution function of h_B. The momentum q of the lepton pair is parametrized as

$$q^\mu = (xP_A^+, yP_B^-, q_\perp^1, q_\perp^2). \tag{12}$$

Because the result contains $\delta^2(q_\perp)$ and its derivative, the result should be taken as a tensor distribution, i.e., the $U(1)$-gauge invariance should be understood in the sense of integration. By taking any test function $\mathcal{F}(q_\perp)$ one should have from the invariance

$$\int d^2q_\perp \mathcal{F}(q_\perp) W^{\mu\nu} q_\mu = 0. \tag{13}$$

The result satisfies this equation and hence is gauge invariant. In d-dimensional space-time the result in Eq. (11) remains the same. An interesting observation in deriving the contribution proportional to the derivative of $\delta^2(q_\perp)$ is that the virtual correction to the contribution beyond tree level is completely determined by the correction of the quark form factor [8].

Beyond tree level $W^{\mu\nu}$ contains more contributions with tensor structures different than those at tree level. In principle one can measure various angular distributions of the outgoing lepton to extract different components of $W^{\mu\nu}$. However, this requires large statistics in experiment. It is convenient to use weighted differential cross sections to project out particular angular distributions, which are transverse-spin dependent. In our case, one can construct weighted differential cross sections to extract the spin-dependent parts of $W^{\mu\nu}$. The differential cross section after the integration over the phase space of the lepton pair can be written as

$$\frac{d\sigma}{dQ^2 d^4q} = \frac{1}{2sq^4}\int d\Gamma_{\ell^+\ell^-} L_{\mu\nu} W^{\mu\nu} \delta(q^2 - Q^2),$$
$$d\Gamma_{\ell^+\ell^-} = \frac{d^3k_1}{(2\pi)^3 2k_1^0}\frac{d^3k_2}{(2\pi)^3 2k_2^0}(2\pi)^4\delta^4(k_1 - k_2 - q) \tag{14}$$

with $s = 2P_A^+ P_B^-$ and the leptonic tensor

$$L^{\mu\nu} = 4(k_1^\mu k_2^\nu + k_1^\nu k_2^\mu - k_1\cdot k_2 g^{\mu\nu}). \tag{15}$$

We take the electric charge of quarks and leptons as 1 for simplicity. This charge factor can be easily recovered later in our final results by multiplying the factor $(4\pi\alpha Q_q)^2$ with Q_q as the electric charge of the quark q in the unit of the electric charge of proton.

In this work we consider the weighted differential cross section with the weight function $\mathcal{O}(q, k_1)$ defined as

$$\frac{d\sigma\langle\mathcal{O}(q,k_1)\rangle}{dxdQ^2} = \frac{1}{4Q^4}\int dy d^2q_\perp d\Gamma_{\ell^+\ell^-}\mathcal{O}(q,k_1) \times L_{\mu\nu}W^{\mu\nu}\delta(q^2 - Q^2) \tag{16}$$

with $\mathcal{O}$ as a function of q and k_1. It is clear that the weighted differential cross section with $\mathcal{O} = 1$ is the usual one. We consider two weights named as $\mathcal{O}_{1,2}$. They are

$$\mathcal{O}_1 = \tilde{s}_\perp \cdot q_\perp,$$
$$\mathcal{O}_2 = \tilde{s}_\perp \cdot k_1 k_1 \cdot q_\perp + \frac{1}{20}(2Q^2 - 7q_\perp\cdot q_\perp)\tilde{s}_\perp \cdot q_\perp. \tag{17}$$

At the first look the second term in the weight $\mathcal{O}_2$ takes a strange form. One may only take the first term as a weight. The reason for the choice of $\mathcal{O}_2$ is that the result becomes simpler after the integration of the lepton-pair phase space,

$$\int d\Gamma_{\ell^+\ell^-}\mathcal{O}_2(q,k_1)L_{\mu\nu} = -\frac{A_\Gamma}{2(d^2-1)}Q^4(q_\perp^\mu \tilde{s}_\perp^\nu + q_\perp^\nu \tilde{s}_\perp^\mu + \mathcal{O}(\epsilon)),$$
$$A_\Gamma = \int d\Gamma_{\ell^+\ell^-} 1. \tag{18}$$

Without the second term in $\mathcal{O}_2$ in Eq. (17), the contribution at the order $\mathcal{O}(\epsilon)$ in the above will be at the order $\mathcal{O}(\epsilon^0)$. This makes the end results very lengthy. It should be emphasized that it is important to measure the differential cross section weighted with $\mathcal{O}_2$ because it receives the contributions from the transversity h_1 at tree level, as shown below. Such a measurement should not be difficult in experiment, although $\mathcal{O}_2$ looks more complicated than $\mathcal{O}_1$. The two weighted differential cross sections can be measured more easily than the full differential cross section.

With the defined weight $\mathcal{O}_{1,2}$ it is straightforward to obtain the results for the corresponding weighted differential cross section,

$$\frac{d\sigma\langle\mathcal{O}_1\rangle}{dxdQ^2} = -\frac{A_{\Gamma 1}}{xsQ^2}\frac{1}{8N_c}|s_\perp|^2\int\frac{d\xi_1 d\xi_2}{\xi_1\xi_2}\delta(1-\xi_1)\delta(1-\xi_2) \times\left[\frac{1}{2}(d-4)h_1(x_a)T_F^{(\sigma)}(y_b,y_b) + (d-2)\bar{q}(y_b)T_F(x_a,x_a)\right],$$
$$\frac{d\sigma\langle\mathcal{O}_2\rangle}{dxdQ^2} = -\frac{A_{\Gamma 2}}{xs}\frac{1}{8N_c}|s_\perp|^2\int\frac{d\xi_1 d\xi_2}{\xi_1\xi_2}\delta(1-\xi_1)\delta(1-\xi_2) \times[-(d-2)h_1(x_a)T_F^{(\sigma)}(y_b,y_b) + 2\bar{q}(y_b)T_F(x_a,x_a)], \tag{19}$$

with

$$x_a = \frac{x}{\xi_1}, \qquad y_b = \frac{Q^2}{x\xi_2 s},$$
$$A_{\Gamma 2} = \frac{A_\Gamma}{2(d^2-1)}, \qquad A_{\Gamma 1} = 2A_\Gamma\frac{d-2}{d-1}. \tag{20}$$

These weighted differential cross sections only receive the contributions from the spin-dependent part of $W^{\mu\nu}$. Since

our weights are proportional to $q_\perp$, they only receive the contributions from terms in Eq. (11) proportional to the derivative of $\delta^2(q_\perp)$. It should be noted that there are contributions in which the parton from h_B is a quark. These contributions involve the quark distribution function of h_B and $T_F(-x,-x)$ of h_A. Similar contributions with chirality-odd operators also exist. In this work we do not list these contributions. These contributions can be obtained with the symmetry of charge conjugation.

We study the one-loop corrections to the weighted differential cross sections. Since the weights are proportional to $q_\perp$, the virtual correction is well known as mentioned. We only need then to calculate the real corrections. In the calculations we meet I.R. and collinear divergences. At the end these divergences are either canceled or correctly subtracted. The final results of the one-loop corrections are finite. Because of the subtraction, we note that the contribution proportional to $d-4=-\epsilon$ in the first line of Eq. (19) gives a nonzero contribution at one loop.

III. THE ONE-LOOP CORRECTION I

In this section we study one-loop correction involving chirality-even operators and that involving purely gluonic twist-3 operators. In general, we need to calculate diagrams which have the patten illustrated in Fig. 1. In these diagrams, there is one parton from the hadron h_B participating in the hard scattering represented by the middle bubble. Figure 1 is for the case that the parton from h_B is an antiquark carrying the momentum k_B. The bubble in the middle denotes those diagrams of the hard scattering. After making the collinear expansion for the antiquark from h_B, the contribution like those given in Fig. 1 can be written as

$$W^{\mu\nu}|_{\text{Fig.1}} = \int d^4k_A d^4k dk_B^- \frac{1}{2N_c}\bar{q}(y_b)\frac{1}{2N_c} \times \text{Tr}[\gamma^+\mathcal{H}^{a,\mu\nu\rho}(k_A,k_B,k)\mathcal{M}_g^{a,\rho}(k_A,k)], \quad (21)$$

with $k_B^\mu=(0,y_bP_B^-,0,0)$ and the quark-gluon correlator

$$\mathcal{M}_g^{a,\rho}(k_A,k) = g_s\int\frac{d^4\eta_1 d^4\eta_2}{(2\pi)^8}e^{i\eta_1\cdot k_A+i\eta_2\cdot k} \times\langle h_A|\bar{q}(0)G^{a,\rho}(\eta_2)q(\eta_1)|h_A\rangle. \quad (22)$$

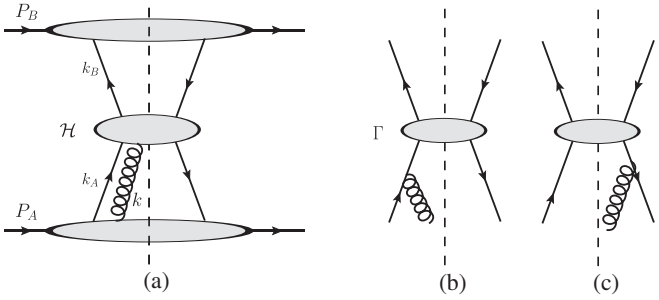

FIG. 1. Diagrams of one-loop correction for SSA. The diagrams in (b) and (c) are not included in (a).

In the above we have already made some approximations to neglect contributions at twist higher than 3.

It is now rather standard to make the collinear expansion related to h_A. Here, one should do the expansion carefully to obtain gauge-invariant results. This has been discussed in detail in [2,21,26]. Since the calculations of twist-3 are now straightforward, we do not give the details about the calculations. One can find the details about how to find gauge-invariant twist-3 contributions in [21,26]. In the relevant twist-3 contributions, there are contributions in which a gluon with the zero momentum from hadrons enters the hard scattering. These contributions are called soft-gluon-pole contributions. It is interesting to note that there is an elegant way to find such contributions [22,23], which we discuss more in detail in Sec. III B. Besides the soft-gluon-pole contributions, there are soft-quark-pole contributions and hard-pole contributions. In the latter the momentum component k^+ of the gluon is not 0 in general.

In the real corrections there is always one parton in the intermediate state in the hard scattering so that the transverse momentum of the virtual photon becomes nonzero. The square of the transverse momentum is given by

$$q_\perp^2 = -q_\perp\cdot q_\perp = \frac{Q^2}{\xi_2}(1-\xi_1)(1-\xi_2). \quad (23)$$

In this section we list our results for the hard-pole contribution in Sec. III A, for the soft-pole contributions in Sec. III B, and for the contributions involving purely gluonic twist-3 operators in Sec. III C. In Sec. III D we perform the subtraction for factorizing the collinear contributions into hadronic matrix elements to avoid a double counting. After the subtraction the results are finite.

A. Hard-pole contributions

The hard-pole contributions are from diagrams given in Figs. 2–4. These diagrams are for the hard scattering represented by $\mathcal{H}$ in Fig. 1. In these diagrams, there is a quark propagator with a short bar. This is to indicate that we only take the absorptive part of the quark propagator in the calculations. The absorptive part is responsible for SSA. To calculate our weighted differential cross section, we need to perform the integration over $q_\perp$. The results after the integration contain I.R. and collinear divergences. These divergences come from the momentum region where the momentum of the massless parton in the intermediate state is soft or collinear to P_A or to P_B. We use the dimensional regularization to regularize these soft divergences. In the regularization the dimension of the space-time is $d=4-\epsilon$ and the dimension of the transverse space is $2-\epsilon$. A scale μ_c related to the soft divergences is introduced. The calculations are tedious but straightforward.

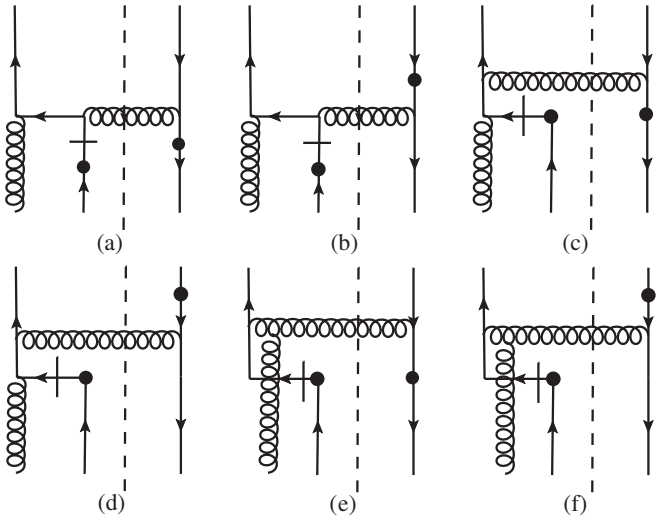

FIG. 2. Diagrams of the hard-pole contributions. The black dots denote the insertion of the electromagnetic current operators in $W^{\mu\nu}$.

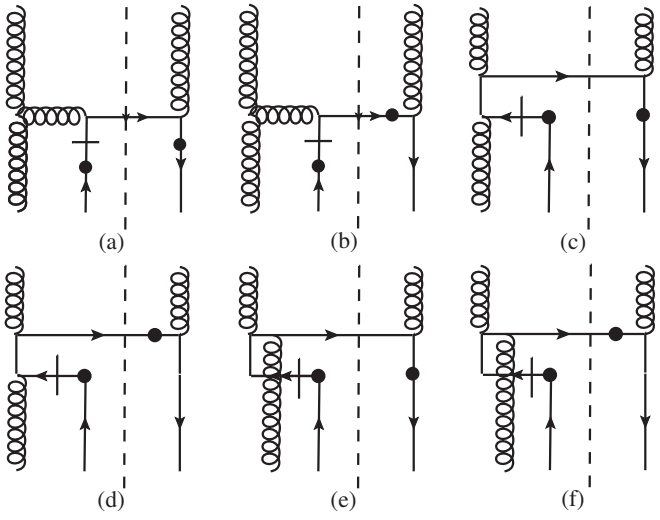

FIG. 3. Diagrams of the hard-pole contributions with a gluon from h_B.

We use the following notations in our work:

$$F_D = \left(\frac{4\pi\mu_c^2}{Q^2}\right)^{\epsilon/2}\frac{1}{\Gamma(1-\epsilon/2)}, \qquad L_2(\xi) = \left(\frac{\ln(1-\xi)}{1-\xi}\right)_+ L_1(\xi) = L_2(\xi) - \frac{\ln\xi}{1-\xi}. \tag{24}$$

The $+$-distributions are standard ones. The hard-pole contribution from diagrams in Fig. 2 is with an antiquark from h_B. The results from these diagrams are

$$\begin{aligned}
\left.\frac{d\sigma\langle\mathcal{O}_1\rangle}{dxdQ^2}\right|_{\text{Fig.2}} &= \frac{|s_\perp|^2 A_{\Gamma 1}}{4xsQ^2}\frac{\alpha_s}{4\pi N_c^2}F_D\int\frac{d\xi_1 d\xi_2}{\xi_1\xi_2}\left\{\bar{q}(y_b)T_F(x_a,z_a)\left[-2N_c^2\left(\frac{2}{\epsilon}\right)^2\delta(1-\xi_1)\delta(1-\xi_2)\right.\right.\\
&\quad + \delta(1-\xi_1)(N_c^2+\xi_2-1)\frac{2}{\epsilon}\frac{(1+\xi_2^2)}{(1-\xi_2)_+} + \delta(1-\xi_2)N_c^2\frac{2}{\epsilon}\frac{1+\xi_1}{(1-\xi_1)_+} + \mathcal{A}_{1F}(\xi_1,\xi_2)\Big]\\
&\quad \left.+\bar{q}(y_b)T_\Delta(x_a,z_a)\left(-\delta(1-\xi_2)N_c^2\frac{2}{\epsilon} + \mathcal{A}_{1\Delta}(\xi_1,\xi_2)\right)\right\},\\
\left.\frac{d\sigma\langle\mathcal{O}_2\rangle}{dxdQ^2}\right|_{\text{Fig.2}} &= \frac{|s_\perp|^2 A_{\Gamma 2}}{4xs}\frac{\alpha_s}{4\pi N_c^2}F_D\int\frac{d\xi_1 d\xi_2}{\xi_1\xi_2}\left\{\bar{q}(y_b)T_F(x_a,z_a)\left[-2N_c^2\delta(1-\xi_1)\delta(1-\xi_2)\right.\right.\\
&\quad \times\left(\left(\frac{2}{\epsilon}\right)^2+\frac{2}{\epsilon}\right) + \delta(1-\xi_1)(N_c^2+\xi_2-1)\frac{1+\xi_2^2}{(1-\xi_2)_+}\frac{2}{\epsilon} + \delta(1-\xi_2)N_c^2\frac{1+\xi_1}{(1-\xi_1)_+}\frac{2}{\epsilon} + \mathcal{A}_{2F}(\xi_1,\xi_2)\Big]\\
&\quad \left.+\bar{q}(y_b)T_\Delta(x_a,z_a)\left[-\delta(1-\xi_2)N_c^2\frac{2}{\epsilon} + \mathcal{A}_{2\Delta}(\xi_1,\xi_2)\right]\right\}.
\end{aligned} \tag{25}$$

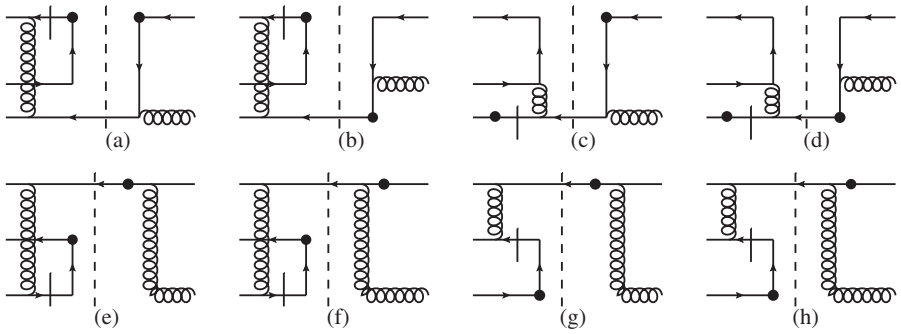

FIG. 4. The diagrams of the hard-pole contributions, where a $q\bar{q}$-pair from h_A enters the hard scattering.

In Eq. (25) we list the divergent contributions explicitly. The terms with the function $\mathcal{A}'s$ are finite. In this and the next section we always give our results in this form. All finite contributions are summed in Sec. V together and the relevant functions are given in the appendix. The variable z_a is

$$z_a = \frac{x\xi_2}{1-\xi_1(1-\xi_2)}. \tag{26}$$

We note that the contributions from Fig. 2 contain a double pole in ϵ.

The hard-pole contributions from diagrams in Fig. 3 are those in which a gluon is a parton from h_B. We denote the twist-2 gluon distribution function of h_B as $G(y)$. The contributions from Fig. 3 are

$$\left.\frac{d\sigma\langle\mathcal{O}_i\rangle}{dxdQ^2}\right|_{\text{Fig.3}} = \frac{|s_\perp|^2 A_{\Gamma i}}{4xsQ^{2(2-i)}}\frac{\alpha_s}{4\pi N_c(N_c^2-1)}F_D\int\frac{d\xi_1 d\xi_2}{\xi_1\xi_2}G(y_b)\Big\{T_F(x_a,z_a)\Big[2C_F\mathcal{B}_{iF}(\xi_1,\xi_2) + \frac{2}{\epsilon}\delta(1-\xi_1)((1-\xi_2)N_c^2-1)(2\xi_2^2-2\xi_2+1)\Big] + 2C_F T_\Delta(x_a,z_a)\mathcal{B}_{i\Delta}(\xi_1,\xi_2)\Big\}, \tag{27}$$

for $i=1,2$. The divergent contributions from Fig. 3 are the same for $i=1,2$. The contributions here contain only a single pole in ϵ associated with T_F.

In the contributions from Figs. 2 and 3 the momentum fractions x_1 for the outgoing quark and x_2 of the incoming quark, as variables of $T_{F,\Delta}(x_1,x_2)$, are always positive. There are contributions in which x_1 or x_2 is negative. In these contributions there is a quark-antiquark pair from h_A entering the hard scattering. These contributions are from Fig. 4. They are

$$\left.\frac{d\sigma\langle\mathcal{O}_i\rangle}{dxdQ^2}\right|_{\text{Fig.4}} = \frac{|s_\perp|^2 A_{\Gamma i}}{4xsQ^{2(2-i)}}\frac{\alpha_s}{4\pi N_c^2}F_D\int\frac{d\xi_1 d\xi_2}{\xi_1\xi_2}\bar{q}(y_b)\Big\{T_F(-x_\xi,z_a)\Big((1-2\xi_1)\delta(1-\xi_2)\frac{2}{\epsilon}+\mathcal{C}_{iF1}(\xi_1,\xi_2)\Big) + T_\Delta(-x_\xi,z_a)\Big(-\delta(1-\xi_2)\frac{2}{\epsilon}+\mathcal{C}_{i\Delta1}(\xi_1,\xi_2)\Big) + T_F(-z_a,x_\xi)\mathcal{C}_{iF2}(\xi_1,\xi_2) + T_\Delta(-z_a,x_\xi)\mathcal{C}_{i\Delta2}(\xi_1,\xi_2)\Big\}, \tag{28}$$

with $x_\xi = x_a - z_a$. We notice that the contributions from those diagrams in the second row of Fig. 4 are finite. The contributions of the first row have the same divergent part for $i=1,2$.

B. Soft-pole contributions

The soft-pole contributions can be soft-gluon-pole or soft-quark-pole contributions. The soft-gluon-pole contributions are from diagrams in Figs. 5 and 6. The soft-quark-pole contributions are from the diagrams in Fig. 7. The soft-quark-pole contributions can be evaluated directly, while it is complicated to calculate the soft-gluon-pole contributions. However, as mentioned, there is an elegant way to obtain the soft-gluon-pole contribution as shown in [22–24]. In our case, the contributions from Fig. 5 can be calculated as discussed in the following.

We consider the contribution to the twist-2 part of $W^{\mu\nu}$ from the partonic process $q(x_aP_A)+\bar{q}(w)\to\gamma^*(q)+g(k_g)$ at tree level. After working out the color factor, the contribution is given by

$$W^{\mu\nu}|_{\text{twist-2}} = \frac{N_c^2-1}{8N_c^2(2\pi)^4}\int\frac{dy_b}{y_b}dx_a\bar{q}(y_b)q(x_a)S^{\mu\nu}(x_aP_A,y_bP_B), \tag{29}$$

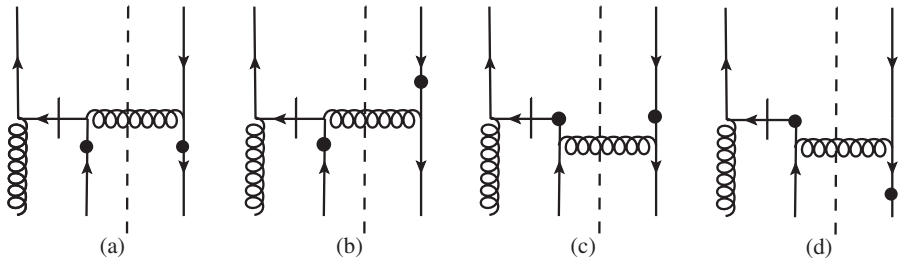

FIG. 5. Diagrams of the soft-gluon-pole contributions.

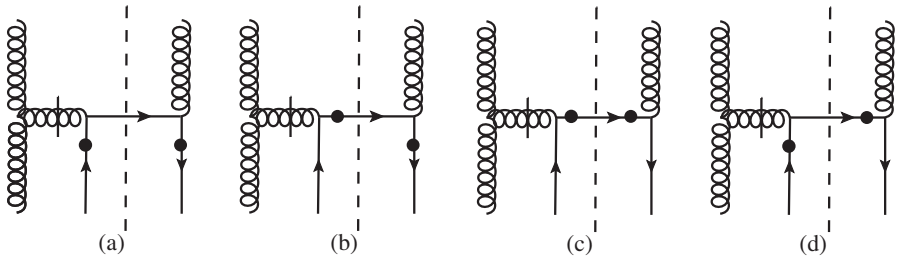

FIG. 6. Diagrams of the soft-gluon-pole contributions with a gluon from h_B.

where $q(x_a)$ is the quark distribution function of h_A. The quantity $S^{\mu\nu}(x_aP_A, w)$ can be simply calculated from the partonic process. Now the soft-pole contribution from Fig. 5 to $W^{\mu\nu}$ at twist-3 can be calculated as [22,23]

$$W^{\mu\nu}|_{\text{Fig.5}} = \frac{-\tilde{s}^\rho}{16N_c^2(2\pi)^4}\int\frac{dy_b}{y_b}dx_a\bar{q}(y_b)T_F(x_a,x_a) \times\left(\frac{\partial}{\partial w_\perp^\rho}-\frac{k_{B\rho}}{k_B^-}\frac{\partial}{\partial w^+}\right)[S^{\mu\nu}(x_aP_A,w)]|_{w^\rho=k_B^\rho}, \quad (30)$$

with $k_B = y_bP_B$. Similar results can also be derived for the twist-3 contribution from Fig. 6.

In the calculation of the soft-gluon contributions to our weighted differential cross sections, the obtained results have not only contributions involving $T_F(x_a, x_a)$, but also contributions involving the derivative of $T_F(x_a, x_a)$ with respect to x_a. These contributions after the integration over $q_\perp$ take the form

$$\int_x^1 dx_a(q_\perp^2)^{-\epsilon/2}f(x_a)\frac{d}{dx_a}T_F(x_a,x_a) = -\int_x^1 dx_aT_F(x_a,x_a)\frac{d}{dx_a}((q_\perp^2)^{-\epsilon/2}f(x_a)), \quad (31)$$

where $q_\perp^2$ is given in Eq. (23). One can perform integration by part to eliminate these terms with the derivative of $T_F(x_a, x_a)$, as shown in the above. Assuming $T_F(1, 1) = 0$ the contribution from the boundary at $x_a = 1$ is 0. The contribution from the boundary at $x_a = x$ is also 0 in d dimension. If we expand the integral in ϵ and then perform the integration by part, the contribution from the boundary at $x_a = x$ is nonzero and should be taken into account. The final results obtained in this way are the same at the considered orders of ϵ, if we perform the integration by part before the expansion in ϵ. We have the contribution from Fig. 5,

$$\begin{aligned}
\left.\frac{d\sigma\langle\mathcal{O}_1\rangle}{dxdQ^2}\right|_{\text{Fig.5}} &= \frac{|s_\perp|^2A_{\Gamma1}}{4xsQ^2}\frac{\alpha_s}{4\pi N_c^2}F_D\int\frac{d\xi_1d\xi_2}{\xi_1\xi_2}\bar{q}(y_b)T_F(x_a,x_a)\left[2\delta(1-\xi_1)\delta(1-\xi_2)\left(\left(\frac{2}{\epsilon}\right)^2-\frac{2}{\epsilon}\right)\right.\\
&\left.-\delta(1-\xi_1)\frac{2}{\epsilon}\frac{(1+\xi_2^2)\xi_2}{(1-\xi_2)_+}-\delta(1-\xi_2)\frac{2}{\epsilon}\frac{1+\xi_1^2}{(1-\xi_1)_+}+\mathcal{D}_1(\xi_1,\xi_2)\right],\\
\left.\frac{d\sigma\langle\mathcal{O}_2\rangle}{dxdQ^2}\right|_{\text{Fig.5}} &= \frac{|s_\perp|^2A_{\Gamma2}}{4xs}\frac{\alpha_s}{4\pi N_c^2}F_D\int\frac{d\xi_1d\xi_2}{\xi_1\xi_2}\bar{q}(y_b)T_F(x_a,x_a)\left[2\delta(1-\xi_1)\delta(1-\xi_2)\left(\frac{2}{\epsilon}\right)^2\right.\\
&\left.-\delta(1-\xi_1)\frac{2}{\epsilon}\frac{\xi_2(1+\xi_2^2)}{(1-\xi_2)_+}-\delta(1-\xi_2)\frac{2}{\epsilon}\frac{1+\xi_1^2}{(1-\xi_1)_+}+\mathcal{D}_2(\xi_1,\xi_2)\right].
\end{aligned} \quad (32)$$

In Eq. (32) there are contributions containing double poles in ϵ. The contributions with the double poles are canceled by those in the virtual corrections.

In the contributions from Fig. 6 the parton from h_B is a gluon. We have

$$\left.\frac{d\sigma\langle\mathcal{O}_i\rangle}{dxdQ^2}\right|_{\text{Fig.6}} = \frac{|s_\perp|^2A_{\Gamma i}}{4xsQ^{2(2-i)}}\frac{\alpha_sN_c}{4\pi(N_c^2-1)}F_D\int\frac{d\xi_1d\xi_2}{\xi_1\xi_2}G(y_b)T_F(x_a,x_a) \times\left[\frac{2}{\epsilon}\delta(1-\xi_1)(2\xi_2^2-2\xi_2+1)\xi_2+\frac{2C_F}{N_c^2}\mathcal{E}_i(\xi_1,\xi_2)\right], \quad (33)$$

for $i = 1, 2$.

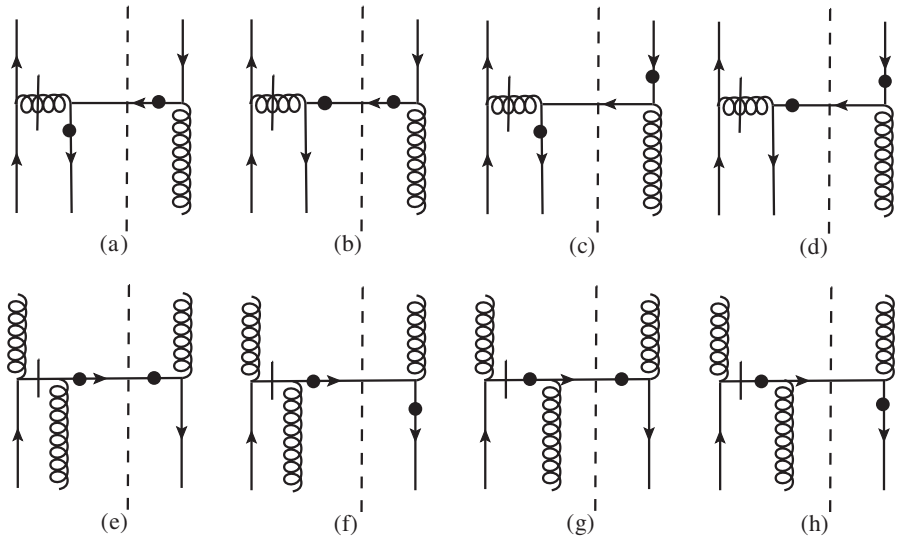

FIG. 7. Diagrams of the soft-quark-pole contributions as one-loop correction for SSA.

As shown in [32], there are soft-quark-pole contributions, in which one of $x_{1,2}$ in $T_{F,\Delta}(x_1,x_2)$ is 0, i.e., a quark or antiquark carrying zero momentum enters a hard scattering. These contributions are from diagrams given in Fig. 7, where in the first four diagrams the parton from h_B is an antiquark, and in the remaining diagrams the parton is a gluon. The method to calculate these contributions is the same as that used for hard-pole contributions in the previous subsection. Interestingly, the results from Fig. 7 can be written in a compact form,

$$\left.\frac{d\sigma\langle\mathcal{O}_i\rangle}{dxdQ^2}\right|_{\text{Fig.7}} = \frac{|s_\perp|^2 A_{\Gamma i}}{4xsQ^{2(2-i)}}\frac{\alpha_s}{4\pi N_c^2}\int\frac{d\xi_1 d\xi_2}{\xi_1\xi_2}\left(\bar{q}(y_b)+\frac{N_c}{N_c^2-1}G(y_b)\right)[T_F(-x_a,0)\mathcal{F}_{iF}(\xi_1,\xi_2) + T_\Delta(-x_a,0)\mathcal{F}_{i\Delta}(\xi_1,\xi_2)], \tag{34}$$

for $i=1,2$. The soft-quark-pole contributions here are finite.

C. Gluonic contribution

The gluonic contributions are those in which only gluons from h_A enter the hard scattering. To calculate these contributions it is convenient to use the notation in [24,27,33] for the twist-3 gluonic matrix elements instead of those given in Eq. (7). In this notation the matrix element of the twist-3 gluonic operator can be parametrized as

$$\frac{1}{P_A^+}g_s i^3\int\frac{d\lambda_1}{2\pi}\frac{d\lambda_2}{2\pi}e^{i\lambda_1 x_1 P_A^+ + i\lambda_2(x_2-x_1)P_A^+}\langle h_A|G^{a,+\alpha}(\lambda_1 n)G^{c,+\gamma}(\lambda_2 n)G^{b,+\beta}(0)|h_A\rangle = \frac{N_c}{(N_c^2-1)(N_c^2-4)}d^{abc}O^{\alpha\beta\gamma}(x_1,x_2) - \frac{i}{N_c(N_c^2-1)}f^{abc}N^{\alpha\beta\gamma}(x_1,x_2), \tag{35}$$

where all indices α, β and γ are transverse. With symmetries the two tensors can be decomposed as

$$\begin{aligned} O^{\alpha\beta\gamma}(x_1,x_2) &= -2i[O(x_1,x_2)g^{\alpha\beta}\tilde{s}_\perp^\gamma + O(x_2,x_2-x_1)g^{\beta\gamma}\tilde{s}_\perp^\alpha + O(x_1,x_1-x_2)g^{\gamma\alpha}\tilde{s}_\perp^\beta],\\ N^{\alpha\beta\gamma}(x_1,x_2) &= -2i[N(x_1,x_2)g^{\alpha\beta}\tilde{s}_\perp^\gamma - N(x_2,x_2-x_1)g^{\beta\gamma}\tilde{s}_\perp^\alpha - N(x_1,x_1-x_2)g^{\gamma\alpha}\tilde{s}_\perp^\beta], \end{aligned} \tag{36}$$

with the properties of the function O and N,

$$O(x_1,x_2)=O(x_2,x_1),\quad O(x_1,x_2)=O(-x_1,-x_2),\quad N(x_1,x_2)=N(x_2,x_1),\quad N(x_1,x_2)=-N(-x_1,-x_2). \tag{37}$$

These functions are related to those defined in Eq. (7) as

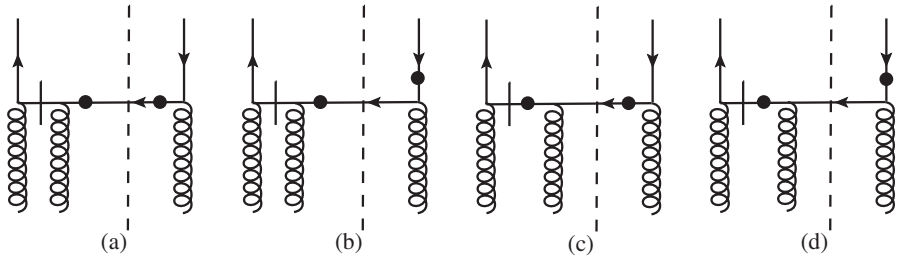

FIG. 8. Diagrams of the gluonic twist-3 contributions.

$$T_G^{(f)}(x_1,x_2) = 2\pi((d-2)N(x_1,x_2) - N(x_2,x_2-x_1) - N(x_1,x_1-x_2)),$$
$$T_G^{(d)}(x_1,x_2) = 2\pi((d-2)O(x_1,x_2) + O(x_2,x_2-x_1) + O(x_1,x_1-x_2)). \quad (38)$$

We use the relations later to express our final results with $T_G^{(f,d)}$. The obtained results can be conveniently expressed with the combinations

$$T_{G+}(x_1,x_2) = T_G^{(f)}(x_1,x_2) + T_G^{(d)}(x_1,x_2),$$
$$T_{G-}(x_1,x_2) = T_G^{(d)}(x_1,x_2) - T_G^{(f)}(x_1,x_2). \quad (39)$$

It should be noted that the relations given in Eq. (38) depend on $d = 4-\epsilon$. The subtraction of the collinear divergences, as discussed in the next subsection, is determined by the evolution of $T_F(x_a,x_a)$. The gluonic part of the evolution derived in the literature is given with T_{G+}. Therefore, for the correct subtraction, one should reexpress the results in terms of T_{G+} and T_{G-} instead of N and O. Then the ϵ-dependence delivers an extra contribution.

With the notation in Eq. (35) there are only four diagrams giving the gluonic contributions. These diagrams are given in Fig. 8. The Bose symmetry between the three gluons is taken into account with the notation for the twist-3 gluonic matrix elements. The gluonic contributions are of soft-pole contributions, in which one gluon carries zero momentum. One can use the method in [22–24] to calculate these contributions in a similar way as explained in the previous subsection. Again, in these contributions we have terms with the derivative on O and N. These terms can be eliminated with integration by part as discussed before. We have the results from Fig. 8,

$$\left.\frac{d\sigma\langle\mathcal{O}_i\rangle}{dxdQ^2}\right|_{\text{Fig.8}} = \frac{\pi|s_\perp|^2 A_{\Gamma i}}{2xsQ^{2(2-i)}}\frac{\alpha_s}{4\pi N_c}F_D\int\frac{d\xi_1 d\xi_2}{\xi_1\xi_2 x_a}\bar{q}(y_b)\left\{\left[-\frac{2}{\epsilon}\delta(1-\xi_2)2(2\xi_1^2-2\xi_1+1)\right]\right.$$
$$\times(O(x_a,x_a)+N(x_a,x_a)+O(x_a,0)-N(x_a,0)) + \frac{1}{N_c}(O(x_a,x_a)$$
$$\left.+N(x_a,x_a))\mathcal{G}_{i+}(\xi_1,\xi_2) + \frac{1}{N_c}(O(x_a,0)-N(x_a,0))\mathcal{G}_{i-}(\xi_1,\xi_2)\right\}. \quad (40)$$

With this result, we have the complete real chirality-even corrections. They are the sum of those results given in Eqs. (25), (27), (28), (32)–(34), and (40).

D. The virtual corrections and the subtraction of the chiral-even contributions

As mentioned, the virtual correction to the contributions with the derivative of $\delta^2(q_\perp)$ in $W^{\mu\nu}$ is determined by the quark form factor as observed in [8]. We call these contributions the derivative contributions. For self-consistence we explain here in detail how the derivative contributions at tree level appear and hence the observation is made.

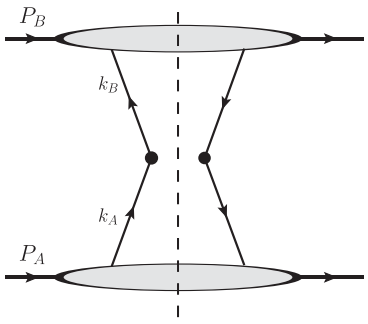

FIG. 9. A tree-level diagram for the contribution to $W^{\mu\nu}$. Lines for gluon exchanges between quark lines and bubbles are implied (see the discussions in text).

The tree-level contributions to $W^{\mu\nu}$ are from Fig. 9, where there are gluon exchanges between the upper (lower) bubble and the quark lines from the lower (upper) bubble. At the leading power, we can neglect all transverse and +-components of momenta of gluons emitted from the upper bubble. At this order, these gluons are polarized in the −-direction. The contributions from the exchange of such gluons can be summed into gauge links along the −-direction. This results in the relevant part from the upper bubble in the contributions at leading power being represented by the antiquark parton distribution function of h_B, i.e., $\bar{q}(y_b)$. With these approximations the tree-level contribution from Fig. 9 with gluon exchanges is given by

$$W^{\mu\nu}|_{\rm Tree} = \sum_{i=0,j=0} \int d^4k_A \left(\prod_{m=1}^{i} d^4k_m\right)\left(\prod_{n=1}^{j} d^4\tilde{k}_n\right)\bar{q}(y_b)\left[\delta^2\left(q_\perp - k_{A\perp} - \sum_{m=1}^{i} k_{m\perp}\right)\mathcal{H}^{\mu\nu\alpha_1\cdots\alpha_i\beta_1\cdots\beta_j}(k_A,\{k_i\},\{\tilde{k}_j\})\right]$$
$$\times \int \frac{d^4\xi}{(2\pi)^4} e^{ik_A\cdot\xi}\left(\prod_{m=1}^{i}\frac{d^4\xi_m}{(2\pi)^4}e^{ik_m\cdot\xi_m}\right)\left(\prod_{n=1}^{j}\frac{d^4\eta_n}{(2\pi)^4}e^{-i\tilde{k}_n\cdot\eta_n}\right)\langle h_A|\bar{\psi}(0)G^{\beta_1}(\eta_1)\cdots G^{\beta_j}(\eta_j)$$
$$\times G^{\alpha_1}(\xi_1)\cdots G^{\alpha_i}(\xi_i)\psi(\xi)|h_A\rangle, \tag{41}$$

where there are exchanges of i gluons in the left part of Fig. 9 and exchanges of j gluons in the right part. The gluon fields in the matrix elements and momenta of partons from the lower bubble scale like $(1,\lambda^2,\lambda,\lambda)$ with $\lambda\sim\Lambda_{\rm QCD}/Q$. For simplicity we omit the color indices in Eq. (41). In our case we can always neglect the − components of gluon momenta and k_A^- in $\mathcal{H}$. This allows us to perform the integrations over the − components of momenta and those of space-time components in +-directions. The contributions with G^- can also be neglected.

To find the contributions at twist-3 we need to perform a collinear expansion in which we expand the $[\cdots]$ in the second line of Eq. (41) in the transverse momenta. We notice that the twist-2 contributions are obtained by taking the leading order in the expansion and taking all gauge fields as G^+'s. After summing the contributions of the exchanged gluons into gauge links in the standard way, the twist-2 contributions are determined by the quark-photon-quark vertex at tree level. In the expansion of the $[\cdots]$ in transverse momenta, one should also expand the δ-function,

$$\delta^2\left(q_\perp - k_{A\perp} - \sum_{m=1}^{i} k_{i\perp}\right)$$
$$= \delta^2(q_\perp) - \left(k^\mu_{A\perp} + \sum_{m=1}^{i} k^\mu_{i\perp}\right)\frac{\partial}{\partial q^\mu_\perp}\delta^2(q_\perp) + \cdots. \tag{42}$$

In the expansion, the first term gives the contributions starting at order of twist-2, while the leading contribution from the second term is at twist-3. It is just the second term which gives the derivative contribution of $W^{\mu\nu}$ at tree level in Eq. (11). The contribution at twist-3 from this term is then obtained by taking all gauge fields as G^+'s and neglecting all transverse parton momenta in $\mathcal{H}$. The calculation is exactly the same as the calculation of twist-2 contributions. The exchange of G^+ gluons can be summed with gauge links along the +-direction. The transverse momenta of partons in the second term can be converted as transverse derivatives acting on parton fields; the final result is then expressed with the correlation function,

$$-iq'_\partial(x)\tilde{s}^\mu_\perp = \int \frac{d\lambda}{4\pi} e^{ix\lambda P_A^+}\langle h_A(P_A,s_\perp)|\bar{\psi}(0)\mathcal{L}_n$$
$$\times (\lambda n)\gamma^+\partial^\mu_\perp(\mathcal{L}^\dagger{}_n\psi)(\lambda n)|h_A(P_A,s_\perp)\rangle, \tag{43}$$

where $\mathcal{L}_n$ is the gauge link in the +-direction pointing to the past. A detailed derivation from the second term in Eq. (42) to the derivative contributions in Eq. (11) can be found in [8]. It is shown that $q'_\partial(x)$ is related to $T_F(x,x)$ in [8,20]. After summing the contributions of exchanged gluons emitted from bubbles into gauge links, the derivative contribution is determined by the quark-photon-quark vertex, i.e., the quark form factor at tree level.

From the above discussion, it is clear that the derivative contributions are evaluated exactly as the calculation of twist-2 contributions except that we have here the correlation function in Eq. (43) instead of the twist-2 quark distribution of h_A. In Eq. (41) $\mathcal{H}$ are contributions of tree-level diagrams. For the case in which $\mathcal{H}$ contain exchanges of virtual gluons, one can perform the same procedure for the contribution with the second term in Eq. (42). After summing the contributions of exchanged gluons emitted from bubbles into gauge links, the derivative contribution is then determined by the quark form factor containing exchanges of virtual gluons. In the case that there are exchanges of real gluons, i.e., the gluons crossing the cut in Fig. 9, the δ-function in Eq. (41) is integrated out and the derivative contribution is absent. This leads to the observation that the virtual correction to the derivative contribution is determined by the quark form factor. The same

conclusion can also be made for SIDIS. The one-loop calculation of the virtual correction involving T_F for Drell-Yan processes in [15] and for SIDIS in [16] verifies our conclusion explicitly. The above discussion is for the contribution involving chiral-even distributions. The same also holds for the derivative contribution involving chiral-odd distributions.

The one-loop result of the form factor is well known. Therefore, we have for the derivative contributions of $W^{\mu\nu}$ up to one loop

$$W^{\mu\nu}|_{\rm vir} = \frac{1}{4N_c}\{-T_F^{(\sigma)}(y,y)h_1(x)(g_\perp^{\mu\rho}\tilde{s}_\perp^\nu + g_\perp^{\nu\rho}\tilde{s}_\perp^\mu - g_\perp^{\mu\nu}\tilde{s}_\perp^\rho) + 2\bar{q}(y)T_F(x,x)g_\perp^{\mu\nu}\tilde{s}_\perp^\rho\}\frac{\partial\delta^2(q_\perp)}{\partial q_\perp^\rho} \times\left\{1+\frac{\alpha_s C_F}{2\pi}F_D\left[-2\left(\frac{2}{\epsilon}\right)^2-3\left(\frac{2}{\epsilon}\right)-8+\pi^2\right]+\mathcal{O}(\alpha_s^2)\right\}+\cdots, \tag{44}$$

where $\cdots$ stand for those nonderivative terms. It is noted that the one-loop corrections of external legs are included so that the correction does not explicitly depend on the renormalization scale μ because of the conservation of the electromagnetic current. Including the virtual corrections, the tree-level results in Eq. (19) are modified by replacement in Eq. (19),

$$1\to\left\{1+\frac{\alpha_s C_F}{2\pi}F_D\left[-2\left(\frac{2}{\epsilon}\right)^2-3\left(\frac{2}{\epsilon}\right)-8+\pi^2\right]\right\}. \tag{45}$$

We note here that the virtual corrections contain a double-pole contribution in ϵ.

From the results in previous subsections we now add all divergent one-loop chirality-even corrections together. We find the divergent part which can be written as

$$\begin{aligned}\left.\frac{d\sigma\langle\mathcal{O}_1\rangle}{dxdQ^2}\right|_{\rm div} &= \frac{|s_\perp|^2A_{\Gamma 1}}{4xsQ^2}\frac{\alpha_s}{2\pi N_c}F_D\int\frac{d\xi_1 d\xi_2}{\xi_1\xi_2}\frac{2}{\epsilon}\Big\{\delta(1-\xi_1)T_F(x_a,x_a)\\ &\times\left[\frac{1}{2}(2\xi_2^2-2\xi_2+1)G(y_b)+P_{qq}(\xi_2)\bar{q}(y_b)\right]+\delta(1-\xi_2)\bar{q}(y_b)\Big[P_{qq}(\xi_1)T_F(x_a,x_a)\\ &+\frac{N_c}{2(1-\xi_1)}((1+\xi_1)T_F(x_a,x)-(1+\xi_1^2)T_F(x_a,x_a))-N_c\delta(1-\xi_1)T_F(x,x)\\ &-\frac{N_c}{2}T_\Delta(x_a,x)+\frac{1}{2N_c}(1-2\xi_1)T_F(x-x_a,x)-\frac{1}{2N_c}T_\Delta(x-x_a,x)\\ &-\frac{1}{2x_a}(2\xi_1^2-2\xi_1+1)T_{G+}(x_a,x_a)\Big]\Big\},\\ \left.\frac{d\sigma\langle\mathcal{O}_2\rangle}{dxdQ^2}\right|_{\rm div} &= \frac{A_{\Gamma 2}Q^2}{A_{\Gamma_1}}\left.\frac{d\sigma\langle\mathcal{O}_1\rangle}{dxdQ^2}\right|_{\rm div},\end{aligned} \tag{46}$$

with

$$P_{qq}(z)=C_F\left[\frac{1+z^2}{(1-z)_+}+\frac{3}{2}\delta(1-z)\right]. \tag{47}$$

We note that the double-pole terms are canceled. The remaining divergent contributions are with a single pole in ϵ. The divergence in the sum is from the momentum region where the parton in the intermediate states or the exchanged gluon in the virtual correction is collinear to h_A or h_B. There are contributions from the soft gluon in the virtual correction and in the intermediate states. These contributions are proportional to $\delta(1-\xi_1)\delta(1-\xi_2)$.

It should be noted that the contributions from the momentum region, where the parton in the intermediate states is collinear to h_A or h_B, are in fact already included in the hadronic matrix elements of the tree-level results given in Eq. (19). To avoid a double counting we should consistently subtract the collinear contributions in the one-loop correction.

We make a replacement in the tree-level results in Eq. (19),

$$\begin{aligned}T_F(x,x)&\to T_F(x,x)-\Delta T_F(x,x),\\ \bar{q}(y)&\to\bar{q}(y)-\Delta\bar{q}(y).\end{aligned} \tag{48}$$

With the replacement in the tree-level results we have the following quantities at the one-loop accuracy:

$$\Delta\frac{d\sigma\langle\mathcal{O}_1\rangle}{dxdQ^2}=\frac{A_{\Gamma 1}(2-\epsilon)|s_\perp|^2}{8xsQ^2N_c}\int\frac{d\xi_1 d\xi_2}{\xi_1\xi_2}\delta(1-\xi_1)\delta(1-\xi_2)(\bar q(y_b)\Delta T_F(x_a,x_a)+\Delta\bar q(y_b)T_F(x_a,x_a)),$$
$$\Delta\frac{d\sigma\langle\mathcal{O}_2\rangle}{dxdQ^2}=\frac{A_{\Gamma 2}|s_\perp|^2}{4xsN_c}\int\frac{d\xi_1 d\xi_2}{\xi_1\xi_2}\delta(1-\xi_1)\delta(1-\xi_2)(\bar q(y_b)\Delta T_F(x_a,x_a)+\Delta\bar q(y_b)T_F(x_a,x_a)). \tag{49}$$

For the subtraction we should add the above quantities to the calculated one-loop corrections, where ΔT_F and $\Delta\bar q$ are specified in the following. We have used the dimensional regularization for ultraviolet (U.V.), I.R., and collinear divergence. With the dimensional regularization ΔT_F and $\Delta\bar q$ are determined by the evolution of the renormalization scale μ, respectively. The evolution of $T_F(x,x)$ can be found in [34–39]. We have then

$$\begin{aligned}\Delta T_F(x,x)&=\frac{\alpha_s}{2\pi}\left(-\frac{2}{\epsilon_c}+\ln\frac{e^\gamma\mu^2}{4\pi\mu_c^2}\right)\left\{-N_cT_F(x,x)+\int_x^1\frac{dz}{z}\left[P_{qq}(z)T_F(\xi,\xi)+\frac{N_c}{2}\left(T_\Delta(x,\xi)\right.\right.\right.\\&\quad\left.+\frac{(1+z)T_F(x,\xi)-(1+z^2)T_F(\xi,\xi)}{1-z}\right)+\frac{1}{2N_c}((1-2z)T_F(x,x-\xi)\\&\quad\left.\left.+T_\Delta(x,x-\xi))-\frac{1}{2}\frac{(1-z)^2+z^2}{\xi}T_{G+}(\xi,\xi)\right]\right\}\\&=\frac{\alpha_s}{2\pi}\left(-\frac{2}{\epsilon_c}+\ln\frac{e^\gamma\mu^2}{4\pi\mu_c^2}\right)(\mathcal{F}_q\otimes T_F+\mathcal{F}_{\Delta q}\otimes T_\Delta+\mathcal{F}_g\otimes T_{G+})(x),\\\Delta\bar q(x)&=\frac{\alpha_s}{2\pi}\left(-\frac{2}{\epsilon_c}+\ln\frac{e^\gamma\mu^2}{4\pi\mu_c^2}\right)\int\frac{d\xi}{\xi}\left\{P_{qq}(z)\bar q(\xi)+\frac{1}{2}[z^2+(1-z)^2]G(\xi)\right\}\\&=\frac{\alpha_s}{2\pi}\left(-\frac{2}{\epsilon_c}+\ln\frac{e^\gamma\mu^2}{4\pi\mu_c^2}\right)(P_{qq}\otimes\bar q+P_{qg}\otimes G)(x),\end{aligned} \tag{50}$$

with $z=x/\xi$. Here we define five convolution $\mathcal{F}$'s for short notations. The derivative of $\Delta T_F(x,x)$ with μ gives the evolution kernel of $T_F(x,x)$ derived in [35,37–39]. Adding the contribution for the subtraction in Eq. (49) to the one-loop correction, we find that all divergent contributions with the single pole in ϵ are canceled. Hence, the final results are finite.

Before ending this section, it should be mentioned that only the contributions from Figs. 2, 5, and 6 to the differential cross section weighted with $\mathcal{O}_1$ have been studied in [15], where the integration over x has been performed partly. Compared with ours the results in [15] are incomplete for the chirality-even contributions.

IV. THE ONE-LOOP CORRECTION II

In this section, we consider the real corrections involving twist-3 chirality-odd operators. There are hard-pole and soft-pole contributions. There is no contribution involving the twist-3 purely gluonic matrix elements and twist-2 gluon distribution functions. The contributions at one loop are from diagrams which have the same patten as given in Fig. 1, where the roles of h_A and h_B are exchanged and the direction of quark lines is reversed. Keeping this in mind, the hard-pole contributions are from Figs. 2 and 4. The soft-gluon contributions are from Fig. 5 and the soft-quark-pole contributions are from the diagrams in the first row of Fig. 7. The calculations are similar to those in the last section. Below we only list our results from these diagrams without giving the details about the calculations. In Sec. IV A we give the results from the mentioned diagrams and the virtual corrections. In Sec. IV B we study the subtraction.

A. The unsubtracted contributions

The hard-pole contributions from Fig. 2 are

$$\begin{aligned}\left.\frac{d\sigma\langle\mathcal{O}_1\rangle}{dxdQ^2}\right|_{\text{Fig.2}}&=\frac{|s_\perp|^2A_{\Gamma 1}}{4xsQ^2}\frac{\alpha_s}{4\pi N_c^2}F_D\int\frac{d\xi_1d\xi_2}{\xi_1\xi_2}h_1(x_a)T_F^{(\sigma)}(y_b,y_0)\left(N_c^2\delta(1-\xi_1)\delta(1-\xi_2)\frac{2}{\epsilon}+\mathcal{A}_{1\sigma}(\xi_1,\xi_2)\right),\\\left.\frac{d\sigma\langle\mathcal{O}_2\rangle}{dxdQ^2}\right|_{\text{Fig.2}}&=\frac{|s_\perp|^2A_{\Gamma 2}}{4xs}\frac{\alpha_s}{4\pi N_c^2}F_D\int\frac{d\xi_1d\xi_2}{\xi_1\xi_2}h_1(x_a)T_F^{(\sigma)}(y_b,y_0)\left\{2N_c^2\delta(1-\xi_1)\delta(1-\xi_2)\left(\frac{2}{\epsilon}\right)^2\right.\\&\quad\left.-2N_c^2\frac{2}{\epsilon}\frac{\delta(1-\xi_1)}{(1-\xi_2)_+}-2\xi_1(N_c^2+\xi_1-1)\frac{2}{\epsilon}\frac{\delta(1-\xi_2)}{(1-\xi_1)_+}+\mathcal{A}_{2\sigma}(\xi_1,\xi_2)\right\},\end{aligned} \tag{51}$$

with $y_0=\xi_2y_b$. We note that in the second equation in Eq. (51) there is a term with the double pole in ϵ, while the first equation contains only a single pole in ϵ.

The hard-pole contributions from Fig. 4 are

$$\left.\frac{d\sigma\langle\mathcal{O}_1\rangle}{dxdQ^2}\right|_{\text{Fig.4}} = \frac{|s_\perp|^2 A_{\Gamma 1}}{4xsQ^2}\frac{\alpha_s}{4\pi N_c^2}F_D\int\frac{d\xi_1 d\xi_2}{\xi_1\xi_2}h_1(x_a)(T_F^{(\sigma)}(y_b-y_0,-y_0)\mathcal{B}_{1\sigma 1}(\xi_1,\xi_2)+T_F^{(\sigma)}(y_0,y_0-y_b)\mathcal{B}_{1\sigma 2}(\xi_1,\xi_2)),$$
$$\left.\frac{d\sigma\langle\mathcal{O}_2\rangle}{dxdQ^2}\right|_{\text{Fig.4}} = \frac{|s_\perp|^2 A_{\Gamma 2}}{4xs}\frac{\alpha_s}{4\pi N_c^2}F_D\int\frac{d\xi_1 d\xi_2}{\xi_1\xi_2}h_1(x_a)\Big\{-2\delta(1-\xi_1)T_F^{(\sigma)}(y_0,y_0-y_b)\frac{2}{\epsilon}(1-\xi_2)$$
$$+T_F^{(\sigma)}(y_b-y_0,-y_0)\mathcal{B}_{2\sigma 1}(\xi_1,\xi_2)+T_F^{(\sigma)}(y_0,y_0-y_b)\mathcal{B}_{2\sigma 2}(\xi_1,\xi_2)\Big\}. \tag{52}$$

In Eq. (52) the first equation does not contain a pole in ϵ, while the second equation contains only a single pole in ϵ.

The soft-gluon-pole contributions from Fig. 5 are

$$\left.\frac{d\sigma\langle\mathcal{O}_1\rangle}{dxdQ^2}\right|_{\text{Fig.5}} = \frac{|s_\perp|^2 A_{\Gamma 1}}{4xsQ^2}\frac{\alpha_s}{4\pi N_c^2}F_D\int\frac{d\xi_1 d\xi_2}{\xi_1\xi_2}h_1(x_a)T_F^{(\sigma)}(y_b,y_b)\left(-\delta(1-\xi_1)\delta(1-\xi_2)\frac{2}{\epsilon}+\mathcal{C}_{1\sigma}(\xi_1,\xi_2)\right),$$
$$\left.\frac{d\sigma\langle\mathcal{O}_2\rangle}{dxdQ^2}\right|_{\text{Fig.5}} = \frac{|s_\perp|^2 A_{\Gamma 2}}{4xs}\frac{\alpha_s}{4\pi N_c^2}F_D\int\frac{d\xi_1 d\xi_2}{\xi_1\xi_2}h_1(x_a)T_F^{(\sigma)}(y_b,y_b)\left[-2\delta(1-\xi_1)\delta(1-\xi_2)\left(\left(\frac{2}{\epsilon}\right)^2-\frac{2}{\epsilon}\right)\right.$$
$$\left.+2\xi_2\delta(1-\xi_1)\frac{2}{\epsilon}\frac{1}{(1-\xi_2)_+}+2\xi_1^2\delta(1-\xi_2)\frac{2}{\epsilon}\frac{1}{(1-\xi_1)_+}+\mathcal{C}_{2\sigma}(\xi_1,\xi_2)\right]. \tag{53}$$

In the second equation of Eq. (53) there is a term with the double pole in ϵ.

The soft-quark-pole contributions from the first row of Fig. 7 are

$$\left.\frac{d\sigma\langle\mathcal{O}_i\rangle}{dxdQ^2}\right|_{\text{Fig.7}} = \frac{|s_\perp|^2 A_{\Gamma i}}{4xsQ^{2(i-2)}}\frac{\alpha_s}{4\pi N_c^2}\int\frac{d\xi_1 d\xi_2}{\xi_1\xi_2}h_1(x_a)T_F^{(\sigma)}(0,-y_b)\mathcal{D}_{i\sigma}(\xi_1,\xi_2), \tag{54}$$

for $i=1,2$. These contributions are finite. The complete real corrections are the sum of the results given by Eqs. (51)–(54).

As discussed, the virtual corrections are obtained by the replacement specified with Eq. (45). Therefore, the virtual corrections for the chirality-odd contributions are

$$\left.\frac{d\sigma\langle\mathcal{O}_1\rangle}{dxdQ^2}\right|_{\text{vir}} = -\frac{|s_\perp|^2 A_{\Gamma 1}}{4xsQ^2}\frac{\alpha_s C_F}{2\pi N_c}F_D\int\frac{d\xi_1 d\xi_2}{\xi_1\xi_2}\delta(1-\xi_1)\delta(1-\xi_2)h_1(x_a)T_F^{(\sigma)}(y_b,y_b)\left(\frac{2}{\epsilon}+\frac{3}{2}\right),$$
$$\left.\frac{d\sigma\langle\mathcal{O}_2\rangle}{dxdQ^2}\right|_{\text{vir}} = -\frac{|s_\perp|^2 A_{\Gamma 2}}{4xs}\frac{\alpha_s C_F}{2\pi N_c}F_D\int\frac{d\xi_1 d\xi_2}{\xi_1\xi_2}\delta(1-\xi_1)\delta(1-\xi_2)h_1(x_a)T_F^{(\sigma)}(y_b,y_b)\left(2\left(\frac{2}{\epsilon}\right)^2+\frac{2}{\epsilon}+5-\pi^2\right). \tag{55}$$

Since the tree-level chirality-odd contribution to the differential cross section weighted with $\mathcal{O}_1$ is proportional to ϵ in Eq. (19), the corresponding one-loop virtual correction has only a single pole in ϵ.

B. The subtraction for the chirality-odd contributions

Summing the various contributions, we obtain the divergent part of the one-loop corrections to the chirality-odd contributions,

$$\left.\frac{d\sigma(\mathcal{O}_1)}{dxdQ^2}\right|_{\text{div}} = \frac{2}{\epsilon}\times 0,$$
$$\left.\frac{d\sigma(\mathcal{O}_2)}{dxdQ^2}\right|_{\text{div}} = \frac{|s_\perp|^2 A_{\Gamma 2}}{4xs}\frac{\alpha_s}{4\pi N_c^2}F_D\frac{2}{\epsilon}\int\frac{d\xi_1 d\xi_2}{\xi_1\xi_2}\Big\{h_1(x_a)T_F^{(\sigma)}(y_b,y_b)\delta(1-\xi_1)\delta(1-\xi_2)(3-N_c^2)+\delta(1-\xi_1)h_1(x_a)$$
$$\times\left[-2\frac{1}{(1-\xi_2)_+}(N_c^2T_F^{(\sigma)}(y_b,y)-\xi_2T_F^{(\sigma)}(y_b,y_b))-2(1-\xi_2)T_F^{(\sigma)}(y,y-y_b)\right]$$
$$-\frac{2}{\epsilon}\delta(1-\xi_2)T_F^{(\sigma)}(y_b,y_b)h_1(x_a)(N_c^2-1)\frac{2\xi_1}{(1-\xi_1)_+}\Big\}. \tag{56}$$

We notice that there is no divergence in the chirality-odd contribution to the differential cross section weighted with $\mathcal{O}_1$ in the sum. In the chirality-odd contribution to the differential cross section weighted with $\mathcal{O}_2$ the double-pole terms in ϵ are canceled; the remaining divergence is with the single pole in ϵ.

Similar to the case of the chirality-even contributions, the divergence in the sum is from the momentum region where the parton in the intermediate states or the exchanged gluon in the virtual correction is collinear to h_A or h_B. These collinear contributions are already included in the hadronic matrix elements in the tree-level results. Therefore, a subtraction is needed to avoid double counting.

The subtraction procedure is the same as discussed for the chirality-even contribution. We make the replacement in our tree-level results,

$$T_F^{(\sigma)}(x,x) \to T_F^{(\sigma)}(x,x) - \Delta T_F^{(\sigma)}(x,x), \qquad h_1(x) \to h_1(x) - \Delta h_1(x), \tag{57}$$

and obtain the contributions of the subtraction,

$$\begin{aligned}
\Delta\frac{d\sigma(\mathcal{O}_1)}{dxdQ^2} &= \frac{A_{\Gamma 1}|s_\perp|^2}{8xsQ^2N_c}\left(-\frac{\epsilon}{2}\right)\int\frac{d\xi_1 d\xi_2}{\xi_1\xi_2}\delta(1-\xi_1)\delta(1-\xi_2)(\Delta h_1(x_a)T_F^{(\sigma)}(y_b,y_b)+h_1(x)\Delta T_F^{(\sigma)}(y_b,y_b)),\\
\Delta\frac{d\sigma(\mathcal{O}_2)}{dxdQ^2} &= -\frac{A_{\Gamma 2}|s_\perp|^2(2-\epsilon)}{8xsN_c}\int\frac{d\xi_1 d\xi_2}{\xi_1\xi_2}\delta(1-\xi_1)\delta(1-\xi_2)(\Delta h_1(x_a)T_F^{(\sigma)}(y_b,y_b)+h_1(x)\Delta T_F^{(\sigma)}(y_b,y_b)).
\end{aligned} \tag{58}$$

These contributions should be added to the one-loop corrections in the previous subsection. We notice that the collinear contributions are not always divergent. An example is the case of the chirality-odd contribution given by the first equation in Eq. (56). With the correct factorization this corresponds to the fact that the contribution of the subtraction in the first equation of Eq. (58) is finite at one loop.

Again, $\Delta T_F^{(\sigma)}(x,x)$ and $\Delta h_1(x)$ are determined by their evolution, respectively. The evolution of $T_F^{(\sigma)}$ has been studied in [39–41]. From the evolution we have

$$\begin{aligned}
\Delta T_F^{(\sigma)}(x,x,\mu) &= \frac{\alpha_s}{2\pi}\left(-\frac{2}{\epsilon_c}+\ln\frac{e^\gamma\mu^2}{4\pi\mu_c^2}\right)\left\{-\frac{N_c^2+3}{4N_c}T_F^{(\sigma)}(x,x,\mu)+\int_x^1\frac{dz}{z}\frac{1}{(1-z)_+}\left(N_cT_F^{(\sigma)}(x,\xi)-\frac{z}{N_c}T_F^{(\sigma)}(\xi,\xi)\right)\right.\\
&\left.\quad+\frac{1}{N_c}\int_0^{1-x}d\xi\frac{\xi}{(\xi+x)^2}T_F^{(\sigma)}(x,-\xi)\right\}\\
&= \frac{\alpha_s}{2\pi}\left(-\frac{2}{\epsilon_c}+\ln\frac{e^\gamma\mu^2}{4\pi\mu_c^2}\right)(\mathcal{F}_\sigma\otimes T_F^{(\sigma)})(x),
\end{aligned} \tag{59}$$

with $z=x/\xi$. Taking the derivative of $\Delta T_F^{(\sigma)}(x,x,\mu)$ we obtain the evolution of $T_F^{(\sigma)}(x,x,\mu)$. The evolution of h_1 has been determined in [42]. From the result there we have

$$\begin{aligned}
\Delta h_1(x) &= \frac{\alpha_s}{2\pi}\left(-\frac{2}{\epsilon_c}+\ln\frac{e^\gamma\mu^2}{4\pi\mu_c^2}\right)C_F\int\frac{d\xi}{\xi}\left(\frac{2z}{(1-z)_+}+\frac{3}{2}\delta(1-z)\right)h_1(\xi)\\
&= \frac{\alpha_s}{2\pi}\left(-\frac{2}{\epsilon_c}+\ln\frac{e^\gamma\mu^2}{4\pi\mu_c^2}\right)(P_{\perp q}\otimes h_1)(x).
\end{aligned} \tag{60}$$

As in Sec. III D we define here two convolutions for short notations.

With the given $\Delta T_F^{(\sigma)}$ and Δh_1 in the above one can perform the subtraction with Eq. (58). For the differential cross section weighted with $\mathcal{O}_2$, we realize that all divergent parts with the pole in ϵ are exactly canceled after the subtraction. For the differential cross section weighted with $\mathcal{O}_1$, although there is no collinear divergence, the subtraction is finite here.

V. THE FINITE RESULTS

To sum our results in previous sections, we introduce two functions as the sums of evolutions combined with other distributions,

$$\mathcal{A}(x_a,y_b)=\bar{q}(y_b)(\mathcal{F}_q\otimes T_F+\mathcal{F}_{\Delta q}\otimes T_\Delta+\mathcal{F}_g\otimes T_{G+})(x_a)+T_F(x_a,x_a)(P_{qq}\otimes\bar{q}+P_{qg}\otimes G)(y_b),$$
$$\mathcal{B}(x_a,y_b)=h_1(x_a)(\mathcal{F}_\sigma\otimes T_F^\sigma)(y_b,y_b)+T_F^{(\sigma)}(y_b,y_b)(P_{\perp q}\otimes h_1)(x_a). \tag{61}$$

The various evolutions can be found in Secs. III D and IVB. The constants $A_{\Gamma 1}$ and $A_{\Gamma 2}$ with $d=4$ are

$$A_{\Gamma 1}=\frac{1}{6\pi},\qquad A_{\Gamma 2}=\frac{1}{240\pi}. \tag{62}$$

Our final result for the differential cross section weighted with $\mathcal{O}_1$ is

$$\begin{aligned}\frac{d\sigma\langle\mathcal{O}_1\rangle}{dxdQ^2}=&-\frac{|s_\perp|^2A_{\Gamma 1}}{4xsQ^2N_c}\int\frac{d\xi_1d\xi_2}{\xi_1\xi_2}\left\{\delta(1-\xi_1)\delta(1-\xi_2)[\bar{q}(y_b)T_F(x_a,x_a)-\frac{\alpha_s}{2\pi}\mathcal{A}(x_a,y_b)\ln\frac{e\mu^2}{Q^2}\right.\\&+\frac{\alpha_sC_F}{2\pi}(\pi^2-5)\bar{q}(y_b)T_F(x_a,x_a)+\frac{\alpha_s}{4\pi}(-\mathcal{B}(x_a,y_b)+3C_Fh_1(x_a)T_F^{(\sigma)}(y_b,y_b))]\\&\left.+\frac{\alpha_s}{8\pi}\frac{1}{x_a}\delta(1-\xi_2)(2\xi_1^2-2\xi_1+1)(3T_{G+}(x_a,x_a)-2T_{G-}(x_a,0))\right\}+\left.\frac{d\sigma\langle\mathcal{O}_1\rangle}{dxdQ^2}\right|_F.\end{aligned} \tag{63}$$

The last term stands for the sum of all finite parts in previous sections. The final result for the differential cross section weighted with $\mathcal{O}_2$ is

$$\begin{aligned}\frac{d\sigma\langle\mathcal{O}_2\rangle}{dxdQ^2}=&-\frac{|s_\perp|^2A_{\Gamma 2}}{4xsN_c}\int\frac{d\xi_1d\xi_2}{\xi_1\xi_2}\left\{\delta(1-\xi_1)\delta(1-\xi_2)\left[\bar{q}(y_b)T_F(x_a,x_a)-\frac{\alpha_s}{2\pi}\mathcal{A}(x_a,y_b)\ln\frac{\mu^2}{Q^2}\right.\right.\\&+\frac{\alpha_sC_F}{2\pi}(\pi^2-8)\bar{q}(y_b)T_F(x_a,x_a)-h_1(x_a)T_F^{(\sigma)}(y_b,y_b)+\frac{\alpha_s}{2\pi}\mathcal{B}(x_a,y_b)\ln\frac{e\mu^2}{Q^2}\\&\left.\left.+\frac{\alpha_sC_F}{2\pi}(5-\pi^2)h_1(x_a)T_F^{(\sigma)}(y_b,y_b)\right]+\frac{\alpha_s}{8\pi}\frac{1}{x_a}\delta(1-\xi_2)(2\xi_1^2-2\xi_1+1)\right.\\&\left.\times(3T_{G+}(x_a,x_a)-2T_{G-}(x_a,0))\right\}+\left.\frac{d\sigma\langle\mathcal{O}_2\rangle}{dxdQ^2}\right|_F.\end{aligned} \tag{64}$$

In these results the contribution with the combination $(3T_{G+}-2T_{G-})$ is the extra contribution discussed after Eq. (39). The final results are finite.

The finite parts in the above are given by

$$\begin{aligned}\left.\frac{d\sigma\langle\mathcal{O}_i\rangle}{dxdQ^2}\right|_F=&\frac{\alpha_s|s_\perp|^2A_{\Gamma i}}{16\pi xs(Q^2)^{2-i}N_c^2}\int\frac{d\xi_1d\xi_2}{\xi_1\xi_2}\left\{\bar{q}(y_b)[T_F(x_a,z_a)\mathcal{A}_{iF}(\xi_1,\xi_2)+T_\Delta(x_a,z_a)\mathcal{A}_{i\Delta}(\xi_1,\xi_2)\right.\\&+T_F(-x_\xi,z_a)\mathcal{C}_{iF1}(\xi_1,\xi_2)+T_F(-z_a,x_\xi)\mathcal{C}_{iF2}(\xi_1,\xi_2)+T_\Delta(-x_\xi,z_a)\mathcal{C}_{i\Delta1}(\xi_1,\xi_2)\\&+T_\Delta(-z_a,x_\xi)\mathcal{C}_{i\Delta2}(\xi_1,\xi_2)+T_F(x_a,x_a)\mathcal{D}_i(\xi_1,\xi_2)+\frac{1}{2x_a}\left(\frac{3}{2}T_{G+}(x_a,x_a)-T_{G-}(x_a,0)\right)\\&\times\mathcal{G}_{i+}(\xi_1,\xi_2)+\frac{1}{2x_a}\left(T_{G-}(x_a,0)-\frac{1}{2}T_{G+}(x_a,x_a)\right)\mathcal{G}_{i-}(\xi_1,\xi_2)\Big]\\&+G(y_b)[T_F(x_a,z_a)\mathcal{B}_{iF}(\xi_1,\xi_2)+T_\Delta(x_a,z_a)\mathcal{B}_{i\Delta}(\xi_1,\xi_2)+T_F(x_a,x_a)\mathcal{E}_i(\xi_1,\xi_2)]\\&+\left(\bar{q}(y_b)+\frac{1}{2C_F}G(y_b)\right)[T_F(-x_a,0)\mathcal{F}_{iF}(\xi_1,\xi_2)+T_\Delta(-x_a,0)\mathcal{F}_{i\Delta}(\xi_1,\xi_2)]\\&+h_1(x_a)[T_F^{(\sigma)}(y_b,y_0)\mathcal{A}_{i\sigma}(\xi_1,\xi_2)+T_F^{(\sigma)}(y_b-y_0,-y_0)\mathcal{B}_{i\sigma1}(\xi_1,\xi_2)\\&\left.+T_F^{(\sigma)}(y_0,y_0-y_b)\mathcal{B}_{i\sigma2}(\xi_1,\xi_2)+T_F^{(\sigma)}(y_b,y_b)\mathcal{C}_{i\sigma}(\xi_1,\xi_2)+T_F^{(\sigma)}(0,-y_b)\mathcal{D}_{i\sigma}(\xi_1,\xi_2)]\right\},\end{aligned} \tag{65}$$

with

$$z_a = \frac{x\xi_2}{1-\xi_1(1-\xi_2)}, \quad x_\xi = x_a - z_a, \quad y_0 = \xi_2 y_b. \tag{66}$$

The functions $\mathcal{A}$'s to $\mathcal{G}$'s are given in the appendix.

As discussed in previous sections about subtractions, the evolutions of $T_F(x,x)$, $T_F^{(\sigma)}(x,x)$ and $h_1(x)$ in our short notations are given by

$$\begin{aligned}
\mu\frac{\partial T_F(x,x,\mu)}{\partial\mu} &= \frac{\alpha_s}{\pi}(\mathcal{F}_q \otimes T_F + \mathcal{F}_{\Delta q}\otimes T_\Delta \\
&\quad + \mathcal{F}_g \otimes T_{G+})(x), \\
\mu\frac{\partial T_F^{(\sigma)}(x,x,\mu)}{\partial\mu} &= \frac{\alpha_s}{\pi}(\mathcal{F}_\sigma \otimes T_F^{(\sigma)})(x), \\
\mu\frac{\partial h_1(x,\mu)}{\partial\mu} &= \frac{\alpha_s}{\pi}(P_{\perp q}\otimes h_1)(x).
\end{aligned} \tag{67}$$

The evolution of $T_F(x,x)$ is given in [35,37–39]. The evolution of $T_F^{(\sigma)}$ and h_1 are derived in [39,41] and [42], respectively. With these evolutions and those of the standard parton distribution functions, one can easily verify that our final results do not depend on the renormalization scale μ.

VI. SUMMARY

We have performed one-loop calculations for the two weighted differential cross sections. They are transverse-spin dependent. These differential cross sections are factorized with hadronic matrix elements defined not only with twist-2 operators but also with twist-3 operators. In our results all collinear contributions, which can be divergent, are factorized into hadronic matrix elements. The final results are finite. Our work gives an example of twist-3 factorization at one loop, in particular, an example of the factorization with chirality-odd twist-3 operators for the first time. With our results SSAs can be predicted more precisely than with tree-level results, or one can extract from experiment, e.g. at the RHIC, twist-3 parton distributions more precisely by measuring the two observables studied here. These distributions will help to understand the inner structure of hadrons. Besides twist-3 parton distributions, one can also use our results to extract the twist-2 transversity distribution, which is still not well known.

In this work, the two weighted differential cross sections for SSA are constructed in such a way that their virtual corrections, as discussed in the introduction, are determined by the corrections of the quark form factor. It is noted that one can construct more observables than the two here. The virtual corrections of these observables may not be determined by the quark form factor and can be complicated. We leave the study of one-loop corrections for such observables for the future.

ACKNOWLEDGMENTS

The work is supported by the National Nature Science Foundation of the People's Republic of China (Grants No. 11275244, No. 11675241, and No. 11605195). The partial support from the CAS center for excellence in particle physics (CCEPP) is acknowledged.

APPENDIX FINITE PARTS OF THE HARD COEFFICIENTS

We give here all functions appearing in the finite part of our results in Eq. (65). These functions are

$$\begin{aligned}
\mathcal{A}_{1F}(\xi_1,\xi_2) &= \delta(1-\xi_1)(N_c^2+\xi_2-1)(\xi_2-1-(1+\xi_2^2)L_1(\xi_2)) - \delta(1-\xi_2)N_c^2(1+\xi_1)L_2(\xi_1) - (N_c^2+\tilde{\xi}_2-1) \\
&\quad \cdot\frac{\xi_1+\tilde{\xi}_2^3+\tilde{\xi}_2-1}{\tilde{\xi}_2(\xi_1-1)_+(\xi_2-1)_+}, \mathcal{A}_{1\Delta}(\xi_1,\xi_2) \\
&= \delta(1-\xi_2)N_c^2(1-\xi_1)L_2(\xi_1) - (N_c^2+\tilde{\xi}_2-1)\frac{\xi_1-\tilde{\xi}_2^3+\tilde{\xi}_2-1}{\tilde{\xi}_2(\xi_1-1)_+(\xi_2-1)_+}, \mathcal{A}_{2F}(\xi_1,\xi_2) \\
&= -2N_c^2\delta(1-\xi_1)\delta(1-\xi_2) + \delta(1-\xi_1)\frac{N_c^2+\xi_2-1}{(1-\xi_2)_+}((1+\xi_2^2)(\xi_2-1)L_1(\xi_2)+2\xi_2) \\
&\quad + \delta(1-\xi_2)N_c^2\frac{1+\xi_1}{(1-\xi_1)_+}((\xi_1-1)L_2(\xi_1)+1) - (N_c^2+\tilde{\xi}_2-1)\frac{\xi_1+\tilde{\xi}_2^2}{(\xi_1-1)_+(\xi_2-1)_+}, \mathcal{A}_{2\Delta}(\xi_1,\xi_2) \\
&= \delta(1-\xi_2)N_c^2((1-\xi_1)L_2(\xi_1)-1) - (N_c^2+\tilde{\xi}_2-1)\cdot\frac{\xi_1-\tilde{\xi}_2^2}{(\xi_1-1)_+(\xi_2-1)_+}, \mathcal{B}_{1F}(\xi_1,\xi_2) \\
&= \frac{1}{2C_F}\Big[\delta(1-\xi_1)(N_c^2(1-\xi_2)-1)(-L_1(\xi_2)(1-\xi_2)(2\xi_2^2-2\xi_2+1)+2\xi_2(\xi_2-1)) \\
&\quad + \frac{(1-\tilde{\xi}_2)N_c^2-1}{\tilde{\xi}_2(1-\xi_1)_+}\xi_1(2\xi_1\tilde{\xi}_2-\xi_1\tilde{\xi}_2^2-\xi_1-2\tilde{\xi}_2^3+3\tilde{\xi}_2^2-3\tilde{\xi}_2+1)\Big],
\end{aligned}$$

$$\mathcal{B}_{1\Delta}(\xi_1,\xi_2)=\frac{1}{2C_F}\frac{(1-\tilde{\xi}_2)N_c^2-1}{\tilde{\xi}_2(1-\xi_1)_+}\xi_1(2\xi_1\tilde{\xi}_2-\xi_1\tilde{\xi}_2^2-\xi_1+3\tilde{\xi}_2^2-3\tilde{\xi}_2+1),$$

$$\mathcal{B}_{2F}(\xi_1,\xi_2)=\frac{1}{2C_F}\Bigg[\delta(1-\xi_1)(N_c^2(1-\xi_2)-1)(-(1-\xi_2)(2\xi_2^2-2\xi_2+1)L_1(\xi_2)+(2\xi_2-1)^2)$$
$$-(N_c^2(1-\tilde{\xi}_2)-1)\frac{\xi_1(2\tilde{\xi}_2^2-2\tilde{\xi}_2+1)}{(1-\xi_1)_+}\Bigg],$$

$$\mathcal{B}_{2\Delta}(\xi_1,\xi_2)=\frac{1}{2C_F}(N_c^2(1-\tilde{\xi}_2)-1)\frac{\xi_1(2\tilde{\xi}_2-1)}{(1-\xi_1)_+},$$

$$\mathcal{C}_{1F1}(\xi_1,\xi_2)=(2\xi_1-1)\delta(1-\xi_2)L_2(\xi_1)(1-\xi_1)+\frac{2\xi_1+\tilde{\xi}_2-2}{\tilde{\xi}_2(1-\xi_2)_+}-N_c\frac{\xi_1}{\tilde{\xi}_2^2}(2\xi_1+\tilde{\xi}_2-2)(\tilde{\xi}_2^2-2\tilde{\xi}_2+2),$$

$$\mathcal{C}_{1\Delta1}(\xi_1,\xi_2)=\delta(1-\xi_2)L_2(\xi_1)(1-\xi_1)+\frac{1}{(1-\xi_2)_+}-N_c\frac{\xi_1}{\tilde{\xi}_2}(\tilde{\xi}_2^2-2\tilde{\xi}_2+2),$$

$$\mathcal{C}_{1F2}(\xi_1,\xi_2)=\frac{\xi_1(1-\tilde{\xi}_2)^2(2\xi_1+\tilde{\xi}_2-2)}{\tilde{\xi}_2}+N_c\frac{\xi_1}{\tilde{\xi}_2^2}(2\xi_1+\tilde{\xi}_2-2)(\tilde{\xi}_2^2-2\tilde{\xi}_2+2)$$

$$\mathcal{C}_{1\Delta2}(\xi_1,\xi_2)=-\xi_1(1-\tilde{\xi}_2)^2-N_c\frac{\xi_1}{\tilde{\xi}_2}(\tilde{\xi}_2^2-2\tilde{\xi}_2+2),$$

$$\mathcal{C}_{2F1}(\xi_1,\xi_2)=(2\xi_1-1)\delta(1-\xi_2)(L_2(\xi_1)(1-\xi_1)-1)+\frac{2\xi_1-2\tilde{\xi}_2+1}{(1-\xi_2)_+}-N_c\frac{\xi_1}{\tilde{\xi}_2}(-2\xi_1\tilde{\xi}_2+4\xi_1+\tilde{\xi}_2^2-4\tilde{\xi}_2+2),$$

$$\mathcal{C}_{2\Delta1}(\xi_1,\xi_2)=\delta(1-\xi_2)(L_2(\xi_1)(1-\xi_1)-1)+\frac{2\tilde{\xi}_2-1}{(1-\xi_2)_+}+N_c\frac{\xi_1}{\tilde{\xi}_2}(-2\xi_1(\tilde{\xi}_2-1)-\tilde{\xi}_2^2),$$

$$\mathcal{C}_{2F2}(\xi_1,\xi_2)=\xi_1(1-\tilde{\xi}_2)(2\xi_1-\tilde{\xi}_2+1)+N_c\frac{\xi_1}{\tilde{\xi}_2}(-2\xi_1\tilde{\xi}_2+4\xi_1+\tilde{\xi}_2^2-4\tilde{\xi}_2+2),$$

$$\mathcal{C}_{2\Delta2}(\xi_1,\xi_2)=\xi_1(1-\tilde{\xi}_2)(2\xi_1+\tilde{\xi}_2-1)+N_c\frac{\xi_1}{\tilde{\xi}_2}(-2\xi_1(\tilde{\xi}_2-1)-\tilde{\xi}_2^2),$$

$$\mathcal{D}_1(\xi_1,\xi_2)=\delta(1-\xi_1)\left((1+\xi_2^2)\xi_2L_1(\xi_2)+\frac{1+\xi_2-\xi_2^2+\xi_2^3}{(1-\xi_2)_+}\right)+\delta(1-\xi_2)\left((1+\xi_1^2)L_2(\xi_1)+\frac{1-\xi_1+\xi_1^2+\xi_1^3}{(1-\xi_1)_+}\right)$$
$$+\frac{-\xi_1^2\tilde{\xi}_2+2\xi_1^2+2\xi_1\tilde{\xi}_2^2-2\xi_1+\tilde{\xi}_2^3-2\tilde{\xi}_2^2+2\tilde{\xi}_2}{(1-\xi_1)_+(1-\xi_2)_+},$$

$$\mathcal{D}_2(\xi_1,\xi_2)=\delta(1-\xi_1)((1+\xi_2^2)\xi_2L_1(\xi_2)+1+\xi_2)+\delta(1-\xi_2)((1+\xi_1^2)L_2(\xi_1)-\xi_1(1+\xi_1))$$
$$+\frac{\xi_1^2(2\tilde{\xi}_2-1)+\xi_1(2\tilde{\xi}_2^2-3\tilde{\xi}_2+1)+\tilde{\xi}_2^3-2\tilde{\xi}_2^2+2\tilde{\xi}_2}{(1-\xi_1)_+(1-\xi_2)_+},$$

$$\mathcal{E}_1(\xi_1,\xi_2)=-\frac{N_c^2}{2C_F}\Bigg[\delta(1-\xi_1)((2\xi_2^2-2\xi_2+1)\xi_2(1-\xi_2)L_1(\xi_2)-2\xi_2^3+4\xi_2^2-2\xi_2+1)$$
$$+\frac{1}{(1-\xi_1)_+}(\xi_1^4+\xi_1^3(3\tilde{\xi}_2-5)+\xi_1^2(6\tilde{\xi}_2^2-12\tilde{\xi}_2+8)+\xi_1(2\tilde{\xi}_2^3-8\tilde{\xi}_2^2+10\tilde{\xi}_2-4))\Bigg],$$

$$\mathcal{E}_2(\xi_1,\xi_2)=-\frac{N_c^2}{2C_F}\Bigg[\delta(1-\xi_1)(\xi_2(1-\xi_2)(2\xi_2^2-2\xi_2+1)L_1(\xi_2)-4\xi_2^3+6\xi_2^2-3\xi_2+1)$$
$$+\frac{1}{(1-\xi_1)_+}(\xi_1^4-2\xi_1^3\tilde{\xi}_2+\xi_1^2(5\tilde{\xi}_2^3-2\tilde{\xi}_2-1)+\xi_1\tilde{\xi}_2(2\tilde{\xi}_2^2-7\tilde{\xi}_2+5))\Bigg],$$

$$
\begin{aligned}
\mathcal{F}_{1F}(\xi_1,\xi_2) &= \xi_1(-2\xi_1^2 - 3\xi_1\tilde{\xi}_2 + 6\xi_1 - \tilde{\xi}_2^2 + 5\tilde{\xi}_2 - 5),\\
\mathcal{F}_{1\Delta}(\xi_1,\xi_2) &= \xi_1(\xi_1\tilde{\xi}_2 - 2\xi_1 + \tilde{\xi}_2^2 - 3\tilde{\xi}_2 + 3),\\
\mathcal{F}_{2F}(\xi_1,\xi_2) &= \xi_1(-2\xi_1^2 + 4\xi_1\tilde{\xi}_2 - \xi_1 - \tilde{\xi}_2^2),\\
\mathcal{F}_{2\Delta}(\xi_1,\xi_2) &= \xi_1(\tilde{\xi}_2^2 - \xi_1),\\
\mathcal{G}_{1+}(\xi_1,\xi_2) &= N_c\Big[\delta(1-\xi_2)(2(2\xi_1^2 - 2\xi_1 + 1)(1-\xi_1)L_2(\xi_1) + 4\xi_1^3 - 4\xi_1^2 + 2\xi_1 + 2)\\
&\quad + \frac{1}{(1-\xi_2)_+}(\xi_1^2(8 - 4\tilde{\xi}_2) + \xi_1(8\tilde{\xi}_2 - 12) + 2\tilde{\xi}_2^2 - 8\tilde{\xi}_2 - 8)\Big],\\
\mathcal{G}_{1-}(\xi_1,\xi_2) &= N_c\Big[\delta(1-\xi_2)(2(2\xi_1^2 - 2\xi_1 + 1)(1-\xi_1)L_2(\xi_1) + 8\xi_1^3 - 16\xi_1^2 + 10\xi_1)\\
&\quad + \frac{1}{(1-\xi_2)_+}(\xi_1^2(16 - 12\tilde{\xi}_2) + \xi_1(-8\tilde{\xi}_2^2 + 32\tilde{\xi}_2 - 28) + 10\tilde{\xi}_2^2 - 24\tilde{\xi}_2 + 16)\Big],\\
\mathcal{G}_{2+}(\xi_1,\xi_2) &= N_c\Big[\delta(1-\xi_2)(2(2\xi_1^2 - 2\xi_1 + 1)(1-\xi_1)L_2(\xi_1) + 4\xi_1^3 - 8\xi_1^2 + 6\xi_1)\\
&\quad + \frac{1}{(1-\xi_2)_+}(4\xi_1^2 + \xi_1\tilde{\xi}_2(6\tilde{\xi}_2 - 10) - 4\tilde{\xi}_2^2 + 6\tilde{\xi}_2)\Big],\\
\mathcal{G}_{2-}(\xi_1,\xi_2) &= N_c\Big[\delta(1-\xi_2)(2(2\xi_1^2 - 2\xi_1 + 1)(1-\xi_1)L_2(\xi_1) + 8\xi_1^3 - 20\xi_1^2 + 14\xi_1 - 2)\\
&\quad + \frac{1}{(1-\xi_2)_+}(\xi_1^2(20 - 16\tilde{\xi}_2) + \xi_1(10\tilde{\xi}_2^2 - 6\tilde{\xi}_2 - 8) - 8\tilde{\xi}_2^2 + 10\tilde{\xi}_2)\Big],\\
\mathcal{A}_{1\sigma}(\xi_1,\xi_2) &= N_c^2\delta(1-\xi_1)\left(\delta(1-\xi_2) - \frac{1}{(1-\xi_2)_+}\right) - (N_c^2 + \xi_1 - 1)\delta(1-\xi_2)\frac{\xi_1}{(1-\xi_1)_+},\\
\mathcal{A}_{2\sigma}(\xi_1,\xi_2) &= 2\delta(1-\xi_1)N_c^2(L_1(\xi_2) + 1) + 2\xi_1(N_c^2 + \xi_1 - 1)\left(\delta(1-\xi_2)L_2(\xi_1) + \frac{1}{(1-\xi_1)_+(1-\xi_2)_+}\right),\\
\mathcal{B}_{1\sigma1}(\xi_1,\xi_2) &= \xi_1(1-\xi_1)(\xi_1 + \tilde{\xi}_2 - 1),\\
\mathcal{B}_{1\sigma2}(\xi_1,\xi_2) &= \delta(1-\xi_1)(\xi_2 - 1) + \xi_1(1 - \xi_1 - \tilde{\xi}_2),\\
\mathcal{B}_{2\sigma1}(\xi_1,\xi_2) &= \xi_1^2(-\xi_1 + 2\tilde{\xi}_2 - 1),\\
\mathcal{B}_{2\sigma2}(\xi_1,\xi_2) &= 2\delta(1-\xi_1)((1-\xi_2)^2L_1(\xi_2) + 1) + \frac{\xi_1^2}{(1-\xi_1)_+}(\xi_1 - 2\tilde{\xi}_2 + 1),\\
\mathcal{C}_{1\sigma}(\xi_1,\xi_2) &= \delta(1-\xi_1)\frac{\xi_2}{(1-\xi_2)_+} + \delta(1-\xi_2)\frac{\xi_1^2}{(1-\xi_1)_+},\\
\mathcal{C}_{2\sigma}(\xi_1,\xi_2) &= -2\xi_2\delta(1-\xi_1)\left(\frac{1}{(1-\xi_2)_+} + L_1(\xi_2)\right) - 2\xi_1^2\delta(1-\xi_2)\left(\frac{1}{(1-\xi_1)_+} + L_2(\xi_1)\right) - \frac{\xi_1(3\xi_1\tilde{\xi}_2 - \xi_1 - \tilde{\xi}_2 + 1)}{(1-\xi_1)_+(1-\xi_2)_+},\\
\mathcal{D}_{1\sigma}(\xi_1,\xi_2) &= \xi_1(\xi_1 - 1)(\xi_1 + \tilde{\xi}_2 - 1),\\
\mathcal{D}_{2\sigma}(\xi_1,\xi_2) &= \xi_1^2(\xi_1 - 2\tilde{\xi}_2 + 1).
\end{aligned}
\tag{A1}
$$

The variable $\tilde{\xi}_2$ is given by

$$
\tilde{\xi}_2 = 1 - \xi_1(1-\xi_2). \tag{A2}
$$

[1] A. V. Efremov and O. V. Teryaev, Sov. J. Nucl. Phys. **36**, 142 (1982); Phys. Lett. **150B**, 383 (1985).
[2] J. W. Qiu and G. Sterman, Phys. Rev. Lett. **67**, 2264 (1991); Nucl. Phys. **B378**, 52 (1992); Phys. Rev. D **59**, 014004 (1998).
[3] N. Hammon, O. Teryaev, and A. Schafer, Phys. Lett. B **390**, 409 (1997); D. Boer, P. J. Mulders, and O. V. Teryaev, Phys. Rev. D **57**, 3057 (1998); Nucl. Phys. **B569**, 505 (2000); D. Boer and J. W. Qiu, Phys. Rev. D **65**, 034008 (2002).
[4] J. Zhou and A. Metz, Phys. Rev. D **86**, 014001 (2012).
[5] I. V. Anikin and O. V. Teryaev, Phys. Lett. B **690**, 519 (2010); Eur. Phys. J. C **75**, 184 (2015).
[6] J. P. Ma and G. P. Zhang, J. High Energy Phys. 11 (2012) 156.
[7] G. Re Calegari and P. G. Ratcliffe, Eur. Phys. J. C **74**, 2769 (2014).
[8] J. P. Ma and G. P. Zhang, J. High Energy Phys. 02 (2015) 163.
[9] X. Ji, J. W. Qiu, W. Vogelsang, and F. Yuan, Phys. Rev. Lett. **97**, 082002 (2006); Phys. Rev. D **73**, 094017 (2006).
[10] K. Kanazawa and Y. Koike, Phys. Lett. B **701**, 576 (2011).
[11] J. P. Ma, H. Z. Sang, and S. J. Zhu, Phys. Rev. D **85**, 114011 (2012).
[12] Y. Koike and S. Yoshida, Phys. Rev. D **85**, 034030 (2012).
[13] J. P. Ma and H. Z. Sang, J. High Energy Phys. 04 (2011) 062.
[14] J. P. Ma and H. Z. Sang, J. High Energy Phys. 11 (2008) 090; H. G. Cao, J. P. Ma, and H. Z. Sang, Commun. Theor. Phys. **53**, 313 (2010).
[15] W. Vogelsang and F. Yuan, Phys. Rev. D **79**, 094010 (2009).
[16] Z.-B. Kang, I. Vitev, and H.-X. Xing, Phys. Rev. D **87**, 034024 (2013).
[17] L.-Y. Dai, Z. B. Kang, A. Prokudin, and I. Vitev, Phys. Rev. D **92**, 114024 (2015).
[18] S. Yoshida, Phys. Rev. D **93**, 054048 (2016).
[19] X. Ji and J. Osborne, Nucl. Phys. **B608**, 235 (2001); A. V. Belitsky, X.-D. Ji, W. Lu, and J. Osborne, Phys. Rev. D **63**, 094012 (2001); X.-D. Ji, W. Lu, J. Osborne, and X. T. Song, Phys. Rev. D **62**, 094016 (2000).
[20] A. P. Chen, J. P. Ma, and G. P. Zhang, Phys. Lett. B **754**, 33 (2016).
[21] H. Eguchi, Y. Koike, and K. Tanaka, Nucl. Phys. **B763**, 198 (2007).
[22] Y. Koike and K. Tanaka, Phys. Lett. B **646**, 232 (2007); Y. Koike and K. Tanaka, *ibid.* **668**, 458(E) (2008).
[23] Y. Koike and K. Tanaka, Phys. Rev. D **76**, 011502 (2007).
[24] Y. Koike, K. Tanaka, and S. Yoshida, Phys. Rev. D **83**, 114014 (2011).
[25] J. C. Collins and D. E. Soper, Nucl. Phys. **B194**, 445 (1982).
[26] H. Eguchi, Y. Koike, and K. Tanaka, Nucl. Phys. **B752**, 1 (2006).
[27] X. D. Ji, Phys. Lett. B **289**, 137 (1992).
[28] R. L. Jaffe and X.-D. Ji, Phys. Rev. Lett. **67**, 552 (1991); R. L. Jaffe and X.-D. Ji, Nucl. Phys. **B375**, 527 (1992).
[29] J. Kodaira and K. Tanaka, Prog. Theor. Phys. **101**, 191 (1999).
[30] A. V. Belitsky and D. Mueller, Nucl. Phys. **B503**, 279 (1997).
[31] J. Zhou, F. Yuan, and Z.-T. Liang, Phys. Rev. D **79**, 114022 (2009).
[32] Y. Koike and T. Tomita, Phys. Lett. B **675**, 181 (2009).
[33] H. Beppu, Y. Koike, K. Tanaka, and Y. Yoshida, Phys. Rev. D **82**, 054005 (2010).
[34] Z.-B. Zhang and J. W. Qiu, Phys. Rev. D **79**, 016003 (2009).
[35] V. M. Braun, A. N. Manashov, and B. Pirnay, Phys. Rev. D **80**, 114002 (2009).
[36] J. Zhou, F. Yuan, and Z.-T. Liang, Phys. Rev. D **81**, 054008 (2010).
[37] J. P. Ma and Q. Wang, Phys. Lett. B **715**, 157 (2012).
[38] A. Schafer and J. Zhou, Phys. Rev. D **85**, 117501 (2012).
[39] Z.-B. Kang and J. W. Qiu, Phys. Lett. B **713**, 273 (2012).
[40] A. V. Belitsky, Phys. Lett. B **453**, 59 (1999).
[41] J. P. Ma, Q. Wang, and G. P. Zhang, Phys. Lett. B **718**, 1358 (2013).
[42] W. Vogelsang, Phys. Rev. D **57**, 1886 (1998).